In-street wind direction variability in the vicinity of a busy intersection in central London.

Ahmed A. Balogun[+] (1), Alison S. Tomlin (1), Curtis R. Wood (2), Janet F. Barlow (2), Stephen E. Belcher (2), Robert J. Smalley (1,3), Justin J.N. Lingard (1), Sam J. Arnold (4), Adrian Dobre (2), Alan G. Robins (5), Damien Martin (6), Dudley E. Shallcross (6)*

(1) Energy and Resources Research Institute, SPEME, University of Leeds, Leeds, West Yorkshire LS2 9JT, UK

(2) Department of Meteorology, University of Reading, Earley Gate, P.O. Box 243, Reading, RG6 6BB, UK

(3) Now at Centre for Australian Weather and Climate Research (CAWCR) Bureau of Meteorology GPO Box 1289K Melbourne VIC 3001 Australia

(4) Golder Associates (UK) Ltd, Nottinghamshire, NG12 5BL, UK

(5) EnFlo, Department of Engineering, University of Surrey, Guildford, Surrey GU2 7XH, UK

(6) School of Chemistry, University of Bristol, Bristol, BS8 1TS, UK

*Phone: +44 (0) 113 343 2500

*Fax: +44 (0) 113 246 7310

*Email: A.S.Tomlin@leeds.ac.uk

[+]Current Affiliation:

Department of Meteorology, Federal University of Technology, Akure, PMB 704, Akure, Ondo State, Nigeria

Email: aabalogun@futa.edu.ng

Abstract

Numerous urban field observations have been devoted to understanding the characteristics of flow and turbulence in urban street canyons. However, cities comprise complex road networks incorporating not just idealised street canyons, but realistic geometries including intersections. Street intersections are a second basic element of urban geometry that are critical in dispersion processes. They can also be local hot-spots for a range of traffic-related pollutants due to co-location

of traffic lights causing vehicle acceleration. Flow characteristics within street intersections, and how they combine with the street canyon flows are challenging to model and are still poorly understood. In addition, intersection flow field data are scarce and are only just becoming available. This paper presents results from fast-response wind measurements within and above a busy intersection between two street canyons (Marylebone Road and Gloucester Place) in Westminster, London taken as part of the DAPPLE (Dispersion of Air Pollution and Penetration into the Local Environment; www.dapple.org.uk) 2007 field campaign. The data reported here were collected using ultrasonic anemometers on the roof-top of a building adjacent to the intersection and at two heights on a pair of lamp-posts on opposite sides of the intersection. Site characteristics, data analysis and the variation of intersection flow with above-roof wind direction (θ_{ref}) are discussed. Evidence of both flow channelling and recirculation were identified within the canyon, only a few metres from the intersection for along street and across street roof-top winds respectively. Results also indicate that for oblique roof-top flows, intersection flow is a complex combination of bifurcated channelled flows, recirculation and corner vortices. Asymmetries in local building geometry around the intersection and small changes in background wind direction (changes in 15-minute mean θ_{ref} of 5–10°) were also observed to have profound influences on the behaviour of intersection flow patterns. Consequently, short time-scale variability in background flow direction can lead to highly scattered in-street mean flow angles masking the true multi-modal features of the flow and thus further complicating modelling challenges.

Keywords DAPPLE, Dispersion, Flow bifurcation, Flow channelling, Recirculation, Urban intersection

1. Introduction

Urban areas are susceptible to elevated pollutant concentrations due to anthropogenic activities, traffic densities and dense building arrangements that inhibit the ventilation of pollutants emitted at street level. The urban canopy layer (UCL) refers to the region below the average height of buildings (Oke 1976) and

is subject to emissions from traffic related sources and other anthropogenic activities such as domestic or commercial heating. The roughness sublayer (RSL), in which roughness elements such as buildings and vegetation have a direct influence on flow properties (Raupach et al. 1980) can extend for several tens of metres over typical urban areas (Rotach 1999). Pollution dispersion processes are strongly related to the patterns of flow and turbulence in these layers in the lower atmosphere. Thus, the understanding of pollution dispersion processes for air quality modelling and strategic air quality management requires a detailed understanding of the characteristics of flow and turbulence in both the UCL and the RSL.

In the past two decades, there has been an increased interest in the study of the urban boundary layer, and analysis of urban field experiments (Eliasson et al. 2006; Hanna et al. 2007; Rotach 1995; Rotach et al. 2005; Klein and Clark 2007), numerical modelling (Johnson and Hunter 1999; Macdonald 2000), wind tunnel studies of wind and turbulence profiles (Kastner-Klein and Plate 1999; Kastner-Klein and Rotach 2004; Klein et al. 2007) as well as reviews (Roth 2000; Britter and Hanna 2003; Ahmad et al. 2005; Vardoulakis et al. 2003) can be found in the literature. These studies have demonstrated that when the flow above roof level is parallel to the street, the wind is efficiently channelled along the street for idealised urban canyon geometries. For conditions with a significant above roof flow component which is perpendicular to the street, a shear layer is shed from the upstream building roof and one or more recirculation vortices may form in the street canyon. For oblique roof-level winds, this cross canyon recirculation may combine with a channelled component to induce a helical wind flow through the canyon (Ahmad et al. 2005; Dobre et al. 2005).

Although there is a growing body of data related to flow in non-idealised geometries in real cities, it is still uncertain whether the flow features of the simple idealised urban canyon geometries mentioned above occur in real cases (Dobre et al. 2005; Klein et al. 2007). Wind tunnel measurements (Kastner-Klein and Rotach 2004) indicate that some of these simple flow features can be found in real geometries. Dobre et al. (2005) also showed that a simple model describing the in-street wind angle as a function of along street and cross street flow

components could be used to represent helical flows in a complex street canyon at the DAPPLE site in central London. Longley et al. (2004) showed how streets bordered by buildings of different heights particularly affect the recirculation vortex. The conceptual model of Dobre was further explored by Barlow et al. (2009) and Wood et al. (2009) for asymmetric cases. Boddy et al. (2005) also showed that a recirculation vortex can exist for above-roof winds that are oblique to the canyon axis, in a relatively complex street canyon (this time in York, UK). However, under certain conditions, the influence of side streets caused the cross-street vortex to break down even for above-roof winds with a strong component perpendicular to the canyon. Dixon et al. (2006) compared the field measurements of Boddy with a computational fluid dynamics (CFD) model based on a simple Reynolds Averaged approach. They found that the model represented well the mean wind patterns in such complex canyons, and indicated the presence of corner vortices and flow convergence due to the influence of side streets.

While numerous urban field observations have been devoted to understanding the characteristics of flow and turbulence in urban street canyons (DePaul and Sheih 1986; Nakamura and Oke 1988; Allwine et al. 2004; Eliasson et al. 2006; Hanna et al. 2007; Hanna et al. 2007; Sugawara et al. 2008), cities consist of complex road networks incorporating not just street canyons but asymmetries in geometry as well as intersections. In addition, flow characteristics within street intersections, and how they combine with the adjoining street canyon flows are still poorly understood. Intersections however, form an important part of the urban form and wind tunnel studies have indicated (Robins et al. 2002) that intersections may play a substantial role in the dispersion of passive scalars through networks of urban streets. Data from intersections in real cities are just starting to become available (Arnold et al. 2004; Tomlin et al. 2009; Dobre et al. 2005; Wood et al. 2009) and the analysis of different sites will allow us to evaluate whether canonical behaviour exists at intersections in a similar way to the generic flow features seen in street canyon geometries. In addition, intersections are particularly relevant to air quality studies, since they are often local “hot spots” of traffic related pollutants such as CO and NOx (Scully 1989; Zamurs 1990; Tate et al. 2009) due to emissions generated as vehicles accelerate away from traffic lights. Intersection flow is also challenging to model and sparse information exists

on the flow and dispersion patterns for model evaluation (Scaperdas and Colvile 1999; Scaperdas et al. 2000 and Soulhac et al. 2001).

Recent theoretical and computational developments have begun to set out a framework for understanding the mean flow within urban canopies. Numerical modelling and wind tunnel experiments suggest that intersections play an important role in the dispersion of urban pollutants and that they should be included in such a framework. Given that small asymmetries in geometry or wind direction can lead to very different flow and dispersion patterns within intersections (Robins et al. 2002; Kastner-Klein and Rotach 2004; Klein et al. 2007; Martin et al. 2008; Soulhac et al. 2009 and Carpentieri et al. 2009; Shallcross et al., 2009), it is of interest to study flow patterns around different geometries and under different background wind conditions. To explore the impact of such complexities further, this study focuses on a busy intersection between two street canyons (Marylebone Road and Gloucester Place) in Westminster London and presents data from the Dispersion of Air Pollution and Penetration into the Local Environment (DAPPLE) project 2007 field campaign. The focus of this study is the dependence of the intersection mean flow patterns, and short term variability in in-street wind angle on the prevailing ambient wind direction.

2. Site Description, Experimental Set up and Data Analysis

2.1 Site description

A 6-week DAPPLE project field measurement campaign was conducted in the spring of 2007 between 22 May and 4 July. An overview of the DAPPLE project and comprehensive description of the measurement site and set-up have been presented in Arnold et al. (2004) for the 2003 campaign and Wood et al. (2009) for the 2007 field measurements. Further information is also available at www.dapple.org.uk.

Briefly, the DAPPLE field site was in Westminster, London at the intersection of Marylebone Road and Gloucester Place (51° 31′ 19″ N, 00° 09′ 35″ W; see Fig. 1a). Marylebone Road is a busy seven lane dual carriageway, approximately 38 m wide and orientated west-south-west to east-north-east. Gloucester Place is a three-lane road approximately 20 m wide and with the traffic flow one-way towards the north-north-west. The roads intersect perpendicularly and have a similar vehicle traffic density of approximately 500 vehicles per hour per lane (Scaperdas and Colvile 1999).

With reference to Fig. 1a and the intersection between Marylebone Road and Gloucester Place, the Westminster Council (WC) building (15–19 m) is in quadrant III and has a central clock-tower of small cross-section, but 34 m high. Marathon House (10–14 m) is in quadrant II and has an office tower-block section over 50 m high. Bickenhall Mansions (20–24 m) is in quadrant IV and Dorset House (30–34 m) is in quadrant I. Within the wider study area, as defined by a circle of radius 250 m centred on the intersection, all the main buildings are less than 40 m in height with a mean of 22 m and there are no uninterrupted street canyons greater than 150 m in length. Figs. 1b and 2 show the layout of the building geometries at the intersection and a close-up of the individual buildings to illustrate the complexity of their structure. These become useful in the discussion of the results. Intersection geometries are site-specific and the most prominent deviation of this site from the traditional intersecting street canyon model is the cut-off corner of the Dorset House building quadrant I, (see Figs.1 and 2c) and the differing building heights.

2.2 Instrumentation

Time series data of all three components of the wind vector (u, v and w) acquired by five in-street ultrasonic anemometers (‘sonics’) and a roof-top reference sonic are investigated. Sonic temperature was also measured but the data is not presented here. The sonics were all three-axis, Research-Grade Gill Scientific Instruments (model R3-50). Four sonics were deployed at the intersection at heights of 7.90 m for the top sonics at sites 1 and 2 (see Fig. 1a) and 3.95 m and

4.15 m for the bottom sonics at sites 1 and 2 respectively on two opposite lampposts in the central reservation of the Marylebone Road and Gloucester Place intersection (see Fig. 1a). Another sonic (site 3) was deployed at 4.15m on the lampposts beside the bus stop in front of Dorset House on Marylebone Road. Site 3 has been included here as a street canyon site to contrast with the intersection sites. The sonics were sampled at 10 Hz and each pair was logged with a 12 V DC battery-powered Campbell CR1000 logger. The loggers were time-stamped and synchronized via GPS. The reference roof-top sonic was located on the SW corner of the WC library roof and is marked by R in Fig. 1a. The roof and sonic head heights were 15.5 and 18.4 m respectively and the roof-top data was logged with a laptop via serial/USB ports at 20 Hz. See Figs. 2a and 2c for a view of the locations of the reference sonic and the in-street sonics on Marylebone Road respectively. Overall, analysis of five weeks of data is presented here and despite breaks in sampling to allow for data download and battery exchange, data capture at the reference roof-top and site 1 was 95%. However only 65% data capture was achieved at site 2 due to logger internal power failure problems that were resolved towards the end of the 2007 campaign.

All reported wind directions use a Cartesian vector system with respect to Marylebone Road (Dobre et al. 2005), so that the roof-top reference wind direction (θ_{ref}) is positive anti-clockwise from 0° when the wind blows along Marylebone Road and +90° when the wind is blowing up Gloucester Place; and presented in the wind vector sense (pointing in the downstream flow direction, Fig 1a).

2.3 Quality assurance

The raw data were subject to a quality assurance procedure that first imposed physical limits on the raw data with values outside these limits rejected as spurious and replaced with an error flag. Plots of the probability density function (pdf) of the daily raw files were also produced to allow visual identification of outlying values and problematic data sets. Further quality assurance checks were performed on the raw daily files based on 15-minute statistics and data outside a window of the mean values $\pm$ 3 times the standard deviation were flagged as

outliers (Klein and Clark 2007). Hourly intervals were rejected if outliers were greater than 600 records out of 36,000. Less than 1% of the data was rejected overall.

Fifteen-minute means and other statistics were subsequently generated. The computations have been achieved with Matlab7 and Fortran programmes developed at the Universities of Leeds and Reading. The 15-minute averaging period is a reasonable time scale that accounts for the full range of mean flow dynamics at street level (Smalley et al. 2008). It is also consistent with the spectral analysis of Dobre et al. (2005) at this location that indicated the existence of a broad spectral maximum across scales corresponding to around 1–300 s. Since the spectral maxima correspond to the most energetic time-scales of the flow, they implied that an averaging period of around 10 minutes will give a reasonable picture of the dynamics of the largest scales in the flow. 15 minutes is chosen here for consistency with traffic and pollution measurements to be reported elsewhere.

3. Reference roof-top wind speed and directions

The pdf of the WC library roof-top reference wind direction (θ_{ref}) and horizontal mean wind speed $U_{ref} = (u^2 + v^2)^{0.5}$ and their variation during the DAPPLE 2007 campaign are shown in Fig. 3. The predominant roof-top wind directions during the campaign were either in quadrants I ($0° \leq \theta_{ref} \leq 90°$) or III ($-180° \leq \theta_{ref} \leq -90°$). Moderate wind speeds were recorded during the campaign with mean winds of 1.85 m s^{-1} and a maximum of 4.65 ms^{-1} in these quadrants. Lighter mean winds of much less than 2 m s^{-1} were observed in quadrants II ($90° \leq \theta_{ref} \leq 180°$) and IV ($-90° \leq \theta_{ref} \leq 0°$).

Klein and Clark (2007) suggested that flow within the urban canopy layer is mostly driven by boundary layer dynamics at the average roof level. The chosen reference sonic is therefore located on the nearby library roof in the southwest corner of the Westminster Council building (Fig. 1). This location is the same as the "LIB reference" used in the 2004 DAPPLE campaign reported by Barlow et al. (2009). It is acknowledged that the reference roof-top sonic is in the roughness sublayer and may be influenced by wake effects associated with individual buildings located upwind of the sonic (particularly the towers of Marathon House

and the Westminster Council building). To assess the influence of local obstructions on the reference roof-top wind measurements, the data were compared with data from simultaneous sonic measurements on the 190 m British Telecom (BT) tower, located approximately 1.5 km away to the east of the roof-top site (51° 31′ 17″ N, 00° 08′ 21″ W). There was very good agreement between the British Telecom tower sonic and library roof-top sonic wind direction with a 9.4° veer with height from roof-top to British Telecom tower-top (Wood et al. 2009). Barlow et al. (2009) showed in their analysis of 2004 DAPPLE data (with predominant wind directions similar to the 2007 measurements), that vertical streamline distortions were generally small at the reference roof-top site. They also observed high values of local turbulence intensity centred on roof-top wind directions of –45° and –165° at the library roof-top site, associated with wake interference from upwind buildings. They thus concluded that the library reference roof-top measurements are expected to be a less reliable indicator of the driving flow direction for wind directions centred on –45 and –165°. However, the predominant prevailing winds on the roof-top site for the 2007 DAPPLE field measurements are towards three directions centred on (–120°, 15° and 72.5°) and are not expected to be affected by these wake influences (see Fig. 3).

4. Influence of roof-top wind direction on intersection flow direction

In this section the dependence of the in-street and intersection flow direction patterns on the reference background mean flow direction is presented. In section 4.1 the influence of all background wind sectors on in-street mean flow direction is investigated. This is followed by the discussion of selected directions of interest for closer analysis of mean wind patterns using vector roses, and higher time resolution analysis using pdfs for selected hourly time periods (section 4.2).

4.1 Intersection and in-street mean wind directions

Fig. 4 shows the dependence of the intersection (sites 1 and 2) and canyon (site 3) mean wind directions on the reference roof-top mean wind direction. Plots of in-

street wind directions (θ_{ij}) vs roof-top wind direction (θ_{ref}) for the four intersection sonics and a canyon sonic are presented using 15-minute averages, where i = 1,2,3 at sites 1, 2 and 3, and j = 1,2 for the upper and lower sonics respectively. To illustrate how roof-top wind speed also affects in-street mean wind direction, the data was further segregated with respect to three thresholds of U_{ref}: ♦ U_{ref} < 1.1 m s^{-1}, ♦ 1.1≤ U_{ref} ≤ 2.5 m s^{-1}, and ♦ U_{ref} > 2.5 m s^{-1}. 1.1 m s^{-1} and 2.5 m s^{-1} correspond to the 25th and 75th percentiles respectively.

Site 3 exhibits the non-linear negative relationship between in-street and roof-top wind direction consistent with helical flow (Fig. 4a) as discussed in previous works by Dobre et al. (2005) and Barlow et al. (2009). The recirculated part of the in-street flow leads to a gradual decrease in in-street flow direction as θ_{ref} increases due to flow reversal at the canyon floor. The blue curve on the figure is the fitted simple model of Dobre et al. (2005) which specifies that the along- and across-canyon velocity components are directly proportional to their above roof-level counterparts based on assumptions of helical flow patterns. Fig. 4a shows that the helical flow assumption is reasonable for most θ_{ref} for the DAPPLE site 3 in the London Marylebone Road Canyon, with a combination of flow channelling and flow reversal due to cross canyon re-circulation being present in the flow patterns. It is shown that the complexity of the in-street flow patterns is not fully captured by the model in quadrant I but it gives a reasonable approximation to flow patterns in the other quadrants. Switching (channelling of recirculated weak mean flow in either direction along the street canyon) of the channelled component of the flow for near perpendicular roof-top wind directions, θ_{ref} around +90° and –90°, leads to large scatter in the mean in-street flow direction at site 3. This scatter extends to a wider range of θ_{ref} angles at low wind-speeds where the influence of additional sources of turbulence (e.g. traffic movements) can affect in-street flow patterns.

There are different responses at the intersection sites (1, 2) compared with the canyon site 3 (Fig. 4). Near the intersection of the two street canyons, it can be expected that the flow is dominated by complex interactions of along street channelling from both canyons and across street recirculation flow types (Klein et

al. 2007), as well as the potential influence of corner vortices. Figs. 4b-e show that this additional complexity within the intersection can cause differences in the relationship between roof-top and in-street mean flow direction compared with the in-canyon site. Figs. 4b and 4c do not show the non-linear negative relationship between in-street and roof-top direction of Fig 4a, that was consistent with helical flow. At site 1 lower (Fig 4c), there is some evidence of mean channelling along Gloucester Place ($\theta_{12} \approx +90°$ for $20 < \theta_{ref} < 100$) in addition to that along the main Marylebone Road canyon for ($-20 < \theta_{ref} < 20$). This channelling behaviour is not seen for the upper Site 1 sonic for $20 < \theta_{ref} < 100$, where the flow is well correlated with the reference flow (see Fig 4b). It is also interesting to note that the in-street mean flow directions for $\theta_{ref} \approx -90°$ and $\theta_{ref} \approx +90°$ at site 1 do not exhibit symmetry (i.e. the opposite direction of each other as observed for the reference flows), with a much higher degree of scatter in the in-street mean flow direction for $\theta_{ref} \approx -90°$ compared to $\theta_{ref} \approx +90°$. Particular sectors of interest with regards to scatter are ($-90° \leq \theta_{ref} \leq -120°$) and ($-14° \leq \theta_{ref} \leq +15°$). The scatter is present for all wind speeds and therefore cannot be wholly attributed to external sources of turbulence (vehicle traffic/buoyancy). The geometric features of the intersection site clearly cause complexities in flow patterns that lead to scatter in the mean in-street direction and require further analysis (see following section).

At site 2 (Fig. 4d and 4e), there is also scatter in the mean flow direction, although less than at site 1. Mean channelling along Gloucester Place is not seen at site 2 and might be because the sonics are slightly further into the main canyon than at site 1. Site 2 shows fairly strong mean channelled flows along Marylebone Road but in common with site 1 exhibits some scatter at $\theta_{ref} \approx -90$ to $-120°$. This roof-top flow direction is from the arc on Dorset House in quadrant I which may be a cause of asymmetries in the in-street behaviour. The flow at site 2 however, is more consistent with height than at site 1, and the scatter is not as wide as for site 1 due to the dominance of channelling behaviour.

Fig. 5a shows that the flow at site 3 is dominated by along street channelling for $\theta_{ref} \approx 0°$ and $\approx 180°$ with only very slight updrafts observed for these channelled flows. Across street recirculation occurs for $\theta_{ref} \approx +90°$ and $\approx -90°$ with the sonic

recording strong updrafts and downdrafts depending on whether the site is in the leeward or windward position. Fig. 5b shows the sector averaged cross street resultant wind speed, $(u^2 + w^2)^{0.5}$ which is a measure of the recirculation at the site (Dobre et al. 2005). It shows that stronger across street recirculation exists for flows towards $\theta_{ref} \approx +90°$ compared to flows towards $\theta_{ref} \approx -90°$. Fig. 5 further supports the presence of helical type motion at site 3 as indicated by Fig. 4a.

4.2 Vector rose analysis and short time-scale variability in in-street flow direction

For a better understanding of the resulting intersection flow patterns observed in Fig. 4, sector wind vector rose analysis based on 15-minute mean data and pdf analysis of the raw 10 Hz data were conducted for along-street, perpendicular and oblique mean reference wind sectors. For the wind vector rose plots, the different wind directions recorded by the roof-top anemometer were segregated by wind speed as in Fig. 4. Each wind speed regime was then split into 12 equal sectors of θ_{ref} of 30°. The first sector was centred on $\theta_{ref} = 0°$, thus this sector includes the range $-14° \leq \theta_{ref} \leq +15°$. Space prevents all sectors from being included here and hence the focus is on those sectors that help to describe the main features of the flow variability. In the following discussion, six sectors centred on 0°, +180° (along Marylebone Road), –90°, +90° (perpendicular to Marylebone Road) and –120°, +60° (oblique flow) are considered. For each 15-minute period recorded by the roof-top anemometer, the corresponding period recorded by the intersection anemometers is presented as a wind vector on a vector rose for all six case sectors. In all figures, the length of the vector indicates the 15-minute mean horizontal wind speed. Pdf plots of in-street wind direction are also shown for 1-hour segments of 10 Hz data near the following θ_{ref} sectors (+60°, –90°, +90° and –120°). The 1-hour periods have been selected so that the 15-minute θ_{ref} remains fairly constant throughout the hour i.e. no large-scale variability in roof-top was present. Each 15 minute average is within $\pm$ 15° of the overall mean. The pdf plots help to explain the short time-scale variability in in-street wind direction, which leads to the scatter in mean flow direction.

4.2.1 Along-street mean reference flows

In this section we test the hypothesis that reference flows which are near-parallel to the main canyon, will lead to channelling within the canyon and intersection sites.

Figures 6a and 6b show the wind vector roses for the reference flow and the resultant in-street flow at Site 1 and Site 2. The figures show that when the mean roof-top wind direction is aligned near-parallel to Marylebone Road ($-14° \leq \theta_{ref} \leq +15°$) or ($+166° \leq \theta_{ref} \leq -165°$), flow at Site 1 is predominantly channelled along Marylebone Road. However, Figs. 4b,c show for Site 1 that oblique components of the roof-top forcing winds in the range $+11° \leq \theta_{ref} \leq +15°$ can lead to in-street angles anywhere within the wider sector $+10° \leq \theta_{11,12} \leq +90°$. This could be a result of a type of flow bifurcation where the competition between channelled flows in each adjoining canyon leads to complexities within the intersection. Bifurcation means the splitting (i.e., branching, division or separation), of a main body into two parts. In fluid dynamics it refers to the two-way separation of a stream of an incompressible flow running up against an immovable walls or obstacles at angled/right-angled open-channel junctions or corners. This behaviour is similar to the observation of Klein et al. (2007) in their wind tunnel intersection studies. They reported that for reference wind directions with an oblique angle with respect to both streets, helical flows from both canyons can meet and interact at the intersection. In general the dominant channelling effects will depend on the background wind direction as well as the geometry of the adjoining streets. In some cases they suggest that channelling in one direction may dominate, but in other cases the flow at the intersection can best be described as bifurcation (Klein et al., 2007). Small changes in background wind angle can clearly lead to shifts in the dominant channelled flows, and therefore shifts in the mean wind angle at site 1.

This combination of different channelled flows within a 15-minute average period is likely to explain the scatter in mean in-street flow direction at site 1 (and will be explored further for oblique roof-top angles in the next section). This feature is of potential relevance for pollutant dispersion, since the idealised picture would

indicate that for roof-top channelled flows, in-street channelling in the same mean direction occurs, as indeed it does at the in-canyon site (Fig. 4a). However, at site 1 within the intersection, even small fluctuations in background flow can lead to channelling along the street perpendicular to the mean background flow, thus potentially broadening the spread of traffic-related pollutants from Marylebone Road, even for near-parallel roof-top wind sectors. A reversed, although less pronounced, characteristic is observed for oblique components of the roof-top flow for sector $+166° \leq \theta_{ref} \leq -165°$ as shown in Fig. 6b. Reversed flow was occasionally observed at site 1 for low roof-top wind speeds ($U_{ref} < 1.1$ m s^{-1}). However, this was not common and might have been a signature of the influence of vehicular traffic travelling in the opposite direction to the air flow on Marylebone Road, rather than suggesting the presence of recirculation due to the site geometric features, which may not persist in such low winds (DePaul and Shieh 1986).

At site 2, Figs. 6a and 6b show that the flow was effectively channelled along Marylebone Road for near-parallel roof-top flows from either direction. This is perhaps expected, since site 2 was further into the canyon than site 1 and was constrained to the north and south by tall buildings. No mean flow channelling along Gloucester Place was observed at site 2 even for slightly oblique roof-top flows. There is, however, a slight deflection towards the South/North in the in-street flow angle for both reference flow directions, particularly at the lower sonic level. Soulhac et al. (2009) and Carpentieri et al (2009) reported from their wind tunnel experiments that several effects influence the velocity field within the intersection. They suggest that flow separation at the upstream corners of the side streets (as a result of bifurcation of the oblique components of the reference flow) can lead to the formation of horizontal recirculation zones or corner vortices at the street entrances, which penetrate into the side streets at a distance of the order of the street width. These recirculation zones also appear to extend a small way into the main street and may be responsible for the deflections observed here. This is shown in Fig. 9 that is discussed later in section 4.2.3.

In summary, although straightforward channelling behaviour occurs within the main Marylebone Road canyon, horizontal vortices and potential flow bifurcation

can lead to a greater degree of scatter in the mean in-street flow direction at the intersection sites.

4.2.2 Across-street mean reference flows

In this section we investigate the effect of roof-top flows which are near-perpendicular to the main canyon and therefore parallel to the narrower Gloucester Place.

For roof-top winds which are limited to the sector $+76° \leq \theta_{ref} \leq +105°$, Figs. 4b, 4c and 7a show that in-street flow angles at site 1 (that is much less constrained on either side by tall buildings compared to site 2) can vary from 0° to +180°. Channelling up Gloucester Place (+90°) is present, however, there are a number of occasions where the mean flow angle was in between the two channelled directions. Again a possible reason is the interaction of channelled flows along both Marylebone Road and Gloucester Place for the oblique roof-top sectors $+76° \leq \theta_{ref} \leq +80°$ and $+100° \leq \theta_{ref} \leq +105°$. No mean recirculation was observed perhaps because this site, under this flow regime, is relatively unconstrained by tall buildings for θ_{ref} around +90°. The deflection westward of the channelled components of the flow along Gloucester Place may also be attributed to the possible influence of the potential horizontal vortex at the mouth of the canyon on Marylebone Road due to flow separation as a result of flow bifurcation of oblique flow components as discussed earlier (Soulhac et al. 2009; Carpentieri et al. 2009).

The situation is different at site 2 which is a deep, wide, step-up canyon for this flow regime. Since site 2 is further into the mouth of the canyon than site 1, this reference flow sector might be considered as across canyon (perpendicular to Marylebone Road) for this site. Figs. 4d, 4e and 7a (top right and bottom right) show that the flow in the canyon near the intersection at site 2 is recirculated and might suggest the existence of a cross-canyon vortex structure with the channelled flow component switching in either direction along the canyon on Marylebone Road. Fig. 7a (top right and bottom right) also shows weak flow channelling up Gloucester Place (~ +90°), that may be attributed to the influence of the open arc

on Dorset House (Fig. 1) causing the vortex structure to break down. However, small changes in the roof-top flow from perpendicular can also lead to in-street channelled components along Marylebone Road. The influence of such small-scale variability in roof-top flow will be further explored below.

Figs. 4b, 4c and 7b show that for along-street roof-top flows towards the sector $-104° \leq \theta_{ref} \leq -75°$ along Gloucester Place, the mean flow directions at the intersection sites differ markedly with a much higher degree of scatter from that observed for similar flows towards the sector $+76° \leq \theta_{ref} \leq +105°$, described above. There are clear influences of site asymmetries since a mirror image would be expected in an idealised symmetrical model situation (Soulhac et al. 2009). At site 1 particularly, in-street flow angles are observed in all sectors, despite the mean roof-top direction being constrained to a 30° sector. At higher reference wind speeds, flow at site 1 appears to be mainly between the angles –130° and 30°. At lower wind speeds, some flow reversal is observed. However, flow which appears to be recirculated towards the northerly sectors under slow wind conditions might be flow redirection due to one-way traffic travelling northwards up Gloucester Place as mentioned earlier.

At site 2, we might expect the flow to be across-canyon and possible flow reversal to be observed. Although little direct mean channelling down Gloucester Place (~ -90°), was observed, few positive mean angles indicating recirculation were observed at site 2, Fig. 7b (top right and bottom right) except under low winds. Mean flow appeared to be deflected into quadrant IV along Marylebone road in this situation (Fig. 7b, top right and bottom right) requiring further explanation. Asymmetries in intersection geometry due to the arc in the Dorset House building in quadrant I of the intersection may lead to the observed asymmetries in in-street angles at site 2 for the two opposite perpendicular reference flow situations. Higher time resolution analysis will attempt to unravel this apparently complex flow situation, since such complexities in mean flow angle will clearly affect dispersion mechanisms within the intersection.

Selected pdf analysis was carried out with the raw 10 Hz data where the roof-top mean flow angle was close to +90° and –90°. The pdfs of two selected 1 hour

segments in the sector $-104° \leq \theta_{ref} \leq -75°$ with mean angles +90.3° (red line) and +92.4° (blue line) are shown in Fig. 8a. The figure to the top left corner of Fig. 8a shows the pdf of the roof-top wind direction and illustrates that although the mean angle is close to +90°, a wide range of angles was observed within a 1 hour segment. Therefore, even for mean perpendicular roof-top flows, oblique flows will be common on shorter time-scales. The figure shows predominant channelling up Gloucester Place (~ +90°) and some flow bifurcation into Marylebone Road (~ 0°) for θ_{12} at site 1 (top right corner). This is consistent with observations in the mean in-street flow angle (Fig. 7b).

The pdfs of two selected 1 hour segments in the sector $-104° \leq \theta_{ref} \leq -75°$ with mean angles –89° (red line) and –95° (blue line) are shown in Fig. 8b. The figure to the top left corner of Fig. 8b shows the pdf of the roof-top wind direction and illustrates that although the mean angle is close to –90°, again, a wide range of angles was observed within a 1 hour segment resulting in oblique flows on shorter time-scales. The figure illustrates a broad pdf for θ_{12} at site 1 (top right corner) which is consistent with the large amount of scatter in the mean in-street flow angle (Fig. 7b).

However, certain peaks are present in the pdfs for both sites 1 and 2. Strong peaks exist for $\theta_{12} \approx -90°$ illustrating channelled flow along Gloucester Place, and $\theta_{12} \approx 0°$ illustrating channelled flow along Marylebone Road. While flow channelling along Gloucester Place could be expected to dominate, there is also clear channelling along Marylebone Road at site 1 on short time-scales, suggesting that even slightly oblique components of roof-top flow in this sector can lead to bifurcation type flows. Recirculation flow features led to positive in-street angles and some flow reversal along Gloucester Place. However, these may be associated with flow redirection due to one-way traffic travelling (~ +90°) up Gloucester Place under low wind speed conditions as discussed earlier.

Fig. 8b shows tri-modal behaviour for site 2 with sharp peaks in the pdf located at 0° and –60° and a broad peak between +90° and +180. Therefore even though the mean background flow is down Gloucester Place, strong channelling along Marylebone Road is still possible on short time-scales due to fluctuations in the

background flow. The peak located at –60° is associated with deflected flow to the east-south-east as mentioned earlier. Dobre et al. (2005) also reported a peak at –60° in the pdf at site 2 for reference roof-top winds in the sector $-90° < \theta_{ref} \leq 0°$ observed during the DAPPLE 2003 field campaign. They attributed the flow deflection to the presence of a car park next to the corner of quadrant I at the intersection (Fig. 1) that deflects the flow at negative angles into Marylebone Road. The flow is also less constrained in this quadrant of the intersection due to the arc in the building of Dorset House.

The comparison of the two slightly different roof-top conditions shows that even small changes in the fluctuating background wind direction pdf and mean angle can lead to significant changes in the relative importance of the different flow features and their complexities at the intersection. The 15-minute mean in-street flow angles perhaps obscure these features, which are more clearly shown by the multi-modal pdfs.

4.2.3 Oblique mean reference flows

Oblique flows towards the North (~ +60°)

The results for oblique mean forcing roof-top winds indicate a combination of complex flow types leading to the observed high degree of scatter in mean in-street flow angles shown in Figs. 4b-c. The relative importance of these features will again be explored using wind vector roses and wind direction pdfs for the mean roof-top sectors $46° \leq \theta_{ref} \leq 75°$ and $106° \leq \theta_{ref} \leq 135°$. Wind tunnel flow characterisation of a 1:200 scaled model of the DAPPLE site for the background wind sector centred on the oblique flow angle +51.35° (Carpentieri et al. 2009) is also shown in Fig. 9 and is referred to in the following discussion.

For the sector centred on 60°, Figs. 4b-c, and 10 show that the mean flow angles at site 1 can vary between 0° and +120°, again exhibiting a wider variability in mean direction than the roof-top flow. The pdfs of two selected 1-hour 10 Hz data segments in the sector ($+46° \leq \theta_{ref} \leq +75°$) in Fig. 11 illustrate the reason for this wide range of mean angles. They show two dominant peaks in θ_{12} for channelled flows along Marylebone Road (0°) and at a slight angle to Gloucester place

(115°). The mean flow visualisation from the wind tunnel study in Fig. 9 suggests that for roof-top winds towards ~ +60°, there is interaction within the intersection between channelled flows from each arm. Slight changes in the roof-top direction can lead to different strengths of channelling along each arm of the intersection and the pdfs (Fig. 11) clearly show how small changes in roof-top mean direction and pdf, substantially alter the relative strength of the peaks. More recirculation (i.e. negative in-street angles) and channelling along Marylebone Road (peak around 0°) are observed for the reference mean wind direction θ_{ref} = +55° (blue line) compared with θ_{ref} = +65° (red line) at site 1. The third peak centred around -80° represents some recirculation that has been masked by the 15-minute averaged wind angles. The observed in-street flow patterns highlight the influence of the variability of the reference wind direction on the strength of channelling, bifurcation and recirculation at both intersection sites. Variability in roof-top flow can be enhanced at street level leading to the scatter observed in the mean flow angles for site 1. This variability could have a substantial influence on the amount of pollution that is transported down each of the canyons adjoining the intersection.

Figs. 4d, 4e, and 10 show that mean flow at site 2 generally has a channelled component along Marylebone Road towards 0° but with a turning southwards (0° to about +30°) at the lower sonic level that suggests the presence of a horizontal corner vortex shed by Bickenhall Mansions corner of site 2. The pdfs for site 2 in Fig. 11 show a broad peak from 0° to about +30° due to the influence of the vortex turning the wind from direct channelling. This is in agreement with the results of the wind tunnel flow visualisation studies of Carpentieri et al. (2009) in Fig. 9. They found a dominant horizontal vortex at the Bickenhall Mansions corner (0° to about +30°), and an intermittent horizontal vortex at the Westminster Council building corner of the intersection respectively (Fig. 9). The dominant horizontal vortex at the Bickenhall Mansions corner at site 2 was observed up to a height of 50 mm (10 m full scale) in the wind tunnel simulation (Carpentieri et al. 2009), but was only indicated by the lower sonic measurements (~ 4 m) in the field study. It was not picked up by the upper sonic (~ 8 m) as shown in Fig. 11. This may suggest that the depth of the vortex is not more than 5 m in reality. Soulhac et al. (2009) also reported the observation of such a vortex in their wind

tunnel intersection and flow visualisation studies for oblique reference winds in this sector.

At site 2 the two peaks centred around –80° and 0° in the pdf on the bottom right corner of Fig. 11 represent cross canyon recirculation, and channelling along Marylebone Road respectively. An increase in the frequency of recirculation and channelling along Marylebone Road was also observed for this sector when compared with site 1 and is probably a result of the site being further into the main Marylebone Road canyon.

The results support recent wind tunnel, flow visualisation and CFD investigations for idealised intersection configurations (Klein et al. 2007; Wang and McNamara 2007; Carpentieri et al. 2009; Soulhac et al. 2009). These studies show that for oblique above roof wind directions, interaction between channelling in both street canyons can occur at the intersection, but might also be superimposed by both vertical and horizontal vortex structures. Our data show that recirculation is captured at the upper and lower sonic heights at both sites (see Figs. 4 and 11), but is more dominant at site 2 which lies further within the canyon mouth. For these complex combinations of flow types, the data show that the transition from predominant channelling, bifurcation or recirculation is greatly influenced by small changes in mean roof-top wind direction of the order of 5-10°, as well as small changes in the spatial location of the sonics with respect to the site geometry.

Oblique flows towards the South (~ –120°)

Figs. 4b – c and 12a show the complex mean flow pattern at site 1 that results for the predominant oblique roof-top flow towards the south, centred on –120° (–134° $\leq \theta_{ref} \leq$ –105°). The mean flow angles suggest that this background wind sector leads to flows with a very high degree of scatter and no obvious preferred in-street flow direction. The wind vector roses and pdf analysis reveals that the cause of this flow direction variability at site 1 is the multi-modal nature of the flow (bifurcation, channelling and recirculation), which is further complicated by asymmetries in site geometry and the influence of vehicular traffic for low roof-top wind speeds. At site 1, for higher wind speeds, the flow is predominantly

recirculated at the lower sonic level (Fig. 12). Because the site is unconstrained towards +90°, and depending on the wind angle, this vortex might breakdown causing the flow to be weakly channelled into Marylebone Road and along Gloucester Place towards –90°. At low wind speeds there appears to be a lack of preferred mean flow direction.

The pdf of wind direction for site 1 lower shown in Fig. 13 has quite a broad spread with significant peaks around –90° (channelled flow down Gloucester Place), 0° (channelled flow along Marylebone Road towards 30° – 45° (recirculated flow). The channelling along Marylebone Road towards 0° is perhaps counterintuitive given the mean roof-top direction. However, the roof-top pdfs suggest that although the mean flow angle is centred on angles less than -90°, there are occasions within the 1-hour samples where the wind switched to angles above –90°. These roof-top flows could then be channelled in-street towards the 30° – 45° direction. In contrast, at the upper site there are a number of mean flow vectors (Fig 12) along Marylebone Road towards 180°, which is a more intuitive result given that the channelled component of the background flow is more towards the west. Clearly, short time-scale variability in the roof-top flows enhances rectification of the flow in opposite directions within the intersection.

At Site 2, Figs. 4d-e and 12 show that the flow is also predominantly recirculated, suggesting the presence of an in-canyon helical flow regime. However, the geometry associated with Dorset House may lead to intermittent breakdown of the recirculation vortex, causing flow to be weakly channelled either along Gloucester Place in both directions or along Marylebone Road. The recirculation shows up as the peak in the direction pdf of the site 2 lower sonic, θ_{22} (Fig. 13 bottom right corner) at +120° (recirculation), but broadly encompassing weak channelling along Gloucester Place (+90°) and also channelling along Marylebone Road (180°), with smaller peaks near 0° and 90° showing lesser channelling. .

The two pdfs with mean angles –120° (red line) and –105° (blue line) further illustrate the observed in-street flow patterns and also highlight again the influence of the variability in the reference wind direction on the dominating flow features (channelling, interaction of channelled flows, recirculation) at both

intersection sites. Larger differences between the two in-street pdfs were observed for site 1. For mean $\theta_{ref} = -120°$ (red line), the recirculated flow dominated with a large peak around +45° in the pdf (top-right of Fig 13). A small shift in the mean roof-to angle to $\theta_{ref} = -105°$ (blue line), leads to more channelling both up Marylebone Road (0°) and down Gloucester Place (–75°) suggesting the interaction of channelled flows. The figure shows that the magnitude of channelling within each street is driven by the variability in the reference flow and that the 15-minute averaged mean angles mask the true multi-modal features and unsteadiness in the in-street flow.

Vertical flow angle

Fig. 13 shows the variation of the 15-minute sector-averaged vertical wind angle within the canyon specified by (γ) =atan2(w/U_h)*180/*pi*, where w is vertical velocity and U_h is horizontal velocity. At site 1, updrafts (positive w) dominate the flow with only reference flows along Marylebone Road leading to mean flow with a small vertical angle. For site 1 the largest positive vertical wind angles occur for cross-canyon and oblique roof-top flows ($45° \leq \theta_{ref} \leq 135°$) and ($-45° \geq \theta_{ref} \geq -135°$), indicating that both recirculated flows and the interaction of channelled flows lead to mean updrafts. These updrafts are much stronger at site 1 than at site 2 perhaps because it is nearer the mouth of the intersection. The strong updrafts are consistent with the idea discussed above that for oblique flows, channelled flow down each adjoining street interacts within the intersection. The wind tunnel data (Fig. 9) for $\theta_{ref} = 51.35°$ also supports this interpretation. The data suggest that as well as bifurcating within the intersection, the initial convergence of the flow drives enhanced vertical motion, with stronger flow along Marylebone Road displacing north-south flow along Gloucester Place upwards. This type of behaviour was also observed by Boddy et al. (2005) and Dixon et al. (2006) due to channelling from side-streets in a York street canyon.

In the majority of cases, vertical motion tends to increase with height and wind speeds greater than 1.1 m s^{-1} were observed to be associated with reduced variability in vertical motion at both sites in all quadrants. The behaviour of γ at site 2 in the sector ($45° \leq \theta_{ref} \leq 135°$) is however markedly different from that at

site 1 in the same sector. In this sector reference wind speeds less than 1.1 m s^{-1} are associated with downdrafts at site 2, while higher wind speeds lead to weak updrafts (Fig.13, top right and bottom right corners). This behaviour supports the earlier assertion that recirculation vortices break down at low wind speeds due to the open arc at Dorset House. Nielson (2000) reported similar observation for weak ambient across street and oblique reference winds ($0 \leq U_{ref} \leq 1.4$ m s^{-1}) in a street canyon in Jagtvej, Copenhagen with side streets adjacent to the windward wall opposite the measurement mast. Nielson concluded that under this condition, the ambient wind was too weak to drive the circulation.

Summary of the effects of oblique above-roof reference flow on in-street flow at an intersection

The current field study, and wind tunnel flow visualisation studies of the DAPPLE site (Carpentieri et al. 2009) have revealed some key features of the response of the intersection flow to oblique roof-top reference flows which are illustrated in the schematic diagram in Fig. 14. The figure proposes that flow at the intersection is a complex combination of cross canyon helical vortices, corner vortices, channelling, and the interaction of channelled flows followed by flow bifurcation. All these lead to strong, three-dimensional interactions between the flows coming into the intersection from the adjoining arms. The lofting of the flow due to interaction between different strengths of channelling along adjoining streets of different widths, is illustrated by the change from red to blue in the diagram. Fig. 14 is consistent with the results of the wind tunnel and flow visualisation observations of Carpentieri et al. (2009). They reported that for the oblique roof-top angle studied, the flow within the intersection can be divided in two different zones: one with a prevalence of near 2-dimensional (horizontal) flow that contains site 2, and one with a more complex 3-dimensional flow that contains site 1.

For oblique flows the results can therefore be summarised as follows. The flow within the main canyon is highly turbulent and 3-dimensional, often exhibiting helical vortex type behaviour. At the intersection it interacts with flow from the other arm of the intersection and is deflected upwards ("lofting") as well as being bifurcated i.e. continuing into Marylebone Road, or deflected into Gloucester Place. Small fluctuations in the background wind direction can change the

strength of flow directed into each street, leading to the multi-modal form of short time-scale pdfs of the intersection wind direction. “Mean” in street flow direction does not therefore have the same implications as it does for the main canyon since it often represents the average of bi- or tri-modal distributions. In addition, intermittent vortices can also form at the corners of the intersection which can deflect the flow from straightforward channelling. Recirculation vortices are also possible but are not as dominant as within the main street canyon itself.

5. Conclusions

The analysis of wind direction variability within a busy intersection between two street canyons (Marylebone Road and Gloucester Place) in Westminster, London during the DAPPLE 2007 field campaign has been presented. Site characteristics, data analysis and the variation of intersection flow patterns with roof-top wind direction have been discussed.

Evidence of both flow channelling and recirculation were identified at the in-canyon site for parallel and perpendicular reference flows with respect to Marylebone Road respectively. These features were also observed within the intersection. However, short-term variability in roof-top flow direction was enhanced within the intersection leading to broad scatter of in-street mean flow angles even for these sectors. For oblique roof-top flows with respect to both streets, results suggest that the intersection flow was three dimensional and was a complex combination of interacting channelled flows, flow bifurcation, helical recirculation patterns and corner vortices. The relative strength of these patterns is highly dependent on short-term variation in roof-top flows and even small changes in mean roof-top flow direction can shift the distribution of in-street flow angles substantially. This would heavily influence the near field dispersion of pollutants emitted at street level in the vicinity of the intersection. Flow at the intersection site which was set a few metres back into the main canyon was observed to behave closer to a typical canyon, even though it was not very deep into the canyon. However, the influence of corner vortices was also observed at this site. Strong updrafts were observed at the site directly in the intersection due to the interaction of channelled flows from each adjoining street. The influence of

such updrafts on the dispersion of a traffic related pollutant was recently discussed by Tomlin et al. (2009).

The field study supports recent modelling and wind tunnel intersection studies (Klein et al. 2007; Wang and McNamara 2007; Carpentieri et al. 2009; Soulhac et al. 2009) for oblique reference flows towards the North. However, the behaviour of the intersection flow was observed to be much more complicated for similar southward reference flows with a high degree of variability due mainly to the asymmetry in the intersection building geometry. Further modelling studies would help to unravel this behaviour.

Small changes in roof-top wind direction were found to have profound influences on the behaviour of intersection flow patterns. Consequently, short time-scale variability in background flow direction can lead to highly scattered in-street mean flow angles that mask the true multi-modal features of the flow. Pdf analysis was found to be a useful tool in helping to interpret the relative importance of the different interacting flow features. Flow disturbance by vehicular traffic also appears to increase the flow complexity for low wind conditions.

Acknowledgements

We acknowledge EPSRC and the Home Office for DAPPLE funding. We also thank DAPPLE colleagues, staff at WCCH, Transport for London and the School of Earth and Environment at the University of Leeds.

References

Ahmad MK, Chaudhry KK (2005) Wind tunnel simulation studies on dispersion at urban street canyons and intersections—a review. J Wind Eng Ind Aerodyn 93:697–717

Allwine KJ, Leach MJ, Stockham LW, Shinn JS, Hosker RP, Bowers JF, Pace JC (2004) Overview of Joint Urban 2003—An atmospheric dispersion study in

Oklahoma City. Preprints, Symposium on Planning, Nowcasting, and Forecasting in the Urban Zone, Seattle, WA. AMS, CDROM, J7.1. 9 pp

Arnold S, ApSimon H, Barlow JF, Belcher S, Bell M, Boddy JWD, Britter R, Cheng H, Clark R, Colvile R, Dimitroulopoulou S., Dobre A, Greally B, Kaur S, Knights, A., Lawton T, Makepeace A, Martin D, Neophytou, M, Neville S, Nieuwenhuijsen M, Nickless G, Price C, Robins A, Shallcross D, Simmonds P, Smalley R, Tate J, Tomlin AS, Wang H, Walsh P (2004) Dispersion of air pollution and penetration into the local environment, DAPPLE. Sci Tot Environ 332:139–153

Barlow AF, Dobre A, Smalley RJ, Arnold SJ, Tomlin AS, Belcher SE (2009) Referencing of street-level flows: results from the DAPPLE 2004 campaign in London, UK. Atmos Environ 43:5536–5544

Boddy JWD, Smalley RJ, Dixon NS, Tate JE, Tomlin AS (2005) The spatial variability in concentrations of a traffic-related pollutant in two street canyons in York, UK. Part I: the influence of background winds. Atmos Environ 39:3147–3161

Britter RE, Hanna SR (2003) Flow and dispersion in urban areas. Ann Rev Fluid Mech 35:469–496

Carpentieri M, Robins A, Baldi S (2009) Three-dimensional mapping of wind flow at an urban canyon intersection. Boundary-Layer Meteorol 133:277–296

DePaul FF, Sheih CM (1986) Measurements of wind velocities in a street canyon. Atmos Environ 20:455–459

Dobre A, Arnold SJ, Smalley RJ, Boddy JWD, Barlow JF, Tomlin AS, Belcher SE (2005) Flow field measurements in the in the proximity of an urban in London, UK. Atmos Environ 39:4647–4657

Dixon NS, Boddy JWD, Smalley RJ, Tomlin AS (2006) Evaluation of a turbulent flow and dispersion model in a typical street canyon in York, UK. Atmos Environ 40:958–972

Eliasson I, Offerle B, Grimmond CSB, Lindqvist S (2006) Wind fields and turbulence statistics in an urban street canyon. Atmos Environ 40:1–16

Hanna SR, Brown MJ, Camelli FE, Chan S, Coirier WJ, Hansen OR, Huber AH, Kim S, Reynolds RM (2006) Detailed simulations of atmospheric flow and dispersion in urban downtown areas by computational fluid dynamics (CFD) models—an application of five CFD models to Manhattan. Bull Am Meteorol Soc 87:1713–1726

Hanna SR, White J, Zhou Y (2007) Observed winds, turbulence and dispersion in built-up downtown areas of Oklahoma City and Manhattan. Boundary-Layer Meteorol 125:441–468

Johnson GT, Hunter LJ (1999) Some insights into typical urban canyons airflows. Atmos Environ 33:3991–3999

Kastner-Klein P, Plate EJ (1999) Wind-tunnel study of concentration fields in street canyons. Atmos Environ 33:3973–3979

Kastner-Klein P, Rotach MW (2004) Mean flow and turbulence characteristics in an urban roughness sublayer. Boundary-Layer Meteorol 111:55–84

Klein P, Clark JV (2007) Flow variability in a North American downtown canyon. J App Meteorol Climatol 46:851–877

Klein P, Leitl B, Schatzmann M (2007) Driving physical mechanisms of flow and dispersion in urban canopies. Int J Climatol 27:1887–1907

Longley ID, Gallagher MW, Dorsey JR, Flynn M, Barlow JF (2004) Short-term measurements of airflow and turbulence in two street canyons in Manchester. Atmos Environ 38:69–79

Macdonald RW (2000) Modeling the mean velocity profile in the urban canopy layer. Boundary-Layer Meteorol 97:25–45

Martin D, Price CS, White IR, Nickless G, Dobre A, Shallcross DE (2008) A study of pollutant concentration variability in an urban street under low wind speeds. Atmos Sci Let 9:147–152

NakamuraY, Oke TR (1988) Wind, temperature and stability conditions in an east-west oriented urban canyon. Atmos Environ 22:2691–2700

Nielson M (2000) Turbulent ventilation of a street. Environ Monit Assess 65:389–396

Oke TR (1976) The distinction between canopy and boundary-layer heat island. Atmos 14:269–277

Oke TR (1988) Street design and the urban canopy layer climate. Energy Build 11:103–113

Raupach MR, Thorn AS, Edwards I (1980) A wind-tunnel study of turbulent flow close to regularly arranged rough surfaces. Boundary-Layer Meteorol 18:373–397

Robins A, Savory E, Scaperdas A, Grigoriadis D (2002) Spatial variability and source–receptor relations at a street intersection. Water Air Soil Pollut Focus 2:381–393

Rotach MW (1995) Profiles of turbulence statistics in and above an urban street Canyon. Atmos Environ 29:1473–1486

Rotach MW (1999) On the influence of the urban roughness sublayer on turbulence and dispersion. Atmos Environ 33:4001–4008

Rotach MW, Vogt R, Bernhofer C, Batchvarova E, Christen A, Clappier A, Feddersen B, Gryning SE, Martucci G, Mayer H, Mitev V, Oke TR, Parlow E, Richner H, Roth M, Roulet YA, Ruffieux D, Salmond J, Schatzmann M, Vogt J (2005) BUBBLE—An urban boundary layer meteorology project. Theor Appl Climatol 81:231–261

Roth M (2000) Review of atmospheric turbulence over cities. Q J Roy Meteorol Soc 126:941–990

Scaperdas A, Colvile RN (1999) Assessing the representativeness of monitoring data from an urban intersection site in central London, UK. Atmos Environ 33:661–674

Scaperdas A, Robins AG, Colville RN (2000) Flow visualisation and tracer dispersion experiments at street canyon intersections. Int J Environ Pollut 14:526–537

Sculley RD (1989) Vehicle emission rate analysis for carbon monoxide hot spot modelling. J Air Pollut Control Assoc 39:1334–1343

Shallcross DE, Martin D, Price CS, Nickless G, White IR, Petersson F, Britter RE, Neophytou MK, Tate JE, Tomlin AS, Barlow JF, Robins A (2009) Short range dispersion experiments using fixed and moving sources, Atmos Sci Let 10:59–65

Smalley RJ, Tomlin AS, Dixon NS, Boddy JWD (2008) The influence of background wind direction on the roadside turbulent velocity field within a complex urban street. Q J Roy Meteorol Soc 134:1371–1384

Soulhac L, Mejean P, Perkins R (2001) Modelling the transport and dispersion of pollutants in street canyons. Int J Environ Pollut 16:404–416

Soulhac L, Garbero V, Salizzoni P, Mejean P, Perkins RJ (2009) Flow and dispersion in street intersections. Atmos Environ 43:2981–2996

Sugawara H, Hagishima A, Narita K, Ogawa H, Yamano M (2008) Temperature and wind distribution in an E-W-oriented urban street canyon. Sci Online Let Atmos 4:53–56

Tate J, Ropkins K, Goodman P, Oates C, Chen H, Bell M, Tomlin A, Balogun A, Smalley R (2009) The influence of traffic congestion, synoptic and in-street winds on NO_2 concentrations around a congested intersection: a measurement study. Procs 7th Int Conf on Air Quality – Science and Application, CDROM, 4pp

Tomlin AS, Smalley RJ, Boddy JWD, Tate JE, Arnold SJ, Dobre A, Barlow JF,Belcher SE (2009) A field study of factors influencing the concentrations of a traffic related pollutant in the vicinity of a complex urban junction. Atmos Environ 43:5027–5037

Vardoulakis S, Fisher BEA, Pericleou K, Gonzalez-Flesca N (2003) Modelling air quality in street canyons: a review. Atmos Environ 37:155–182

Wood CR, Arnold SJ, Balogun AA, Barlow JF, Belcher SE, Britter RE, Cheng H, Dobre A, Lingard JJN, Martin D, Neophytou MK, Petersson FK, Robins AG, Shallcross DE, Smalley RJ, Tate JE, Tomlin AS, White IR (2009) Dispersion experiments in central London: The 2007 DAPPLE project. Bull Am Meteorol Soc 90:955–969

Zamurs J (1990) Intersection carbon monoxide modelling. J Air Waste Manag Assoc 40:769–771

Figure captions

Fig. 1a Aerial view of the intersection illustrating the right hand Cartesian coordinate system used. The u and v velocity components are aligned along Marylebone Road and Gloucester Place, respectively. Wind vector angle θ is positive anti-clockwise, 0° when the wind blows along Marylebone Road), 90° when the wind blows up Gloucester Place. Note that these are wind vectors, hence pointing in the direction of flow. The roof-top reference (R), intersection sonics (1 and 2) and in-street sonic (3) sites are marked.

Fig. 1b Bird's eye view of Marylebone Road and Gloucester Place intersection, showing the complexity of the building geometries. The red dots indicate the location of the measurement systems for the data presented here during the DAPPLE 2007 campaign (see also Fig 1a).

Fig. 2 (a) View of roof-top sonic anemometer, (b) Marathon House on the quadrant II corner of the intersection, (c) Dorset House quadrant I corner, (d) Site 3 at the bus stop after the intersection in front of Dorset House, (e) Westminster Council building in quadrant III corner and (f) Bickenhall Mansions in quadrant IV corner. The white circles in (c) show the location of the four intersection sonics and the in-street sonic.

Fig. 3 Probability density function (Pdf) of the 15-minute mean horizontal wind direction and wind-speed distribution at the roof-top reference anemometer: (a) pdf of horizontal wind direction, (b) pdf of horizontal wind speed and (c) 15 minute mean wind direction and wind speeds for the duration of the DAPPLE 2007 campaign. The colour scale represents the data frequency at each point.

Fig. 4 – Plots of 15-minute mean wind directions (θ_{ij}) against roof-top wind direction (θ_{ref}) for the in-street sonics, where i = 1, 2, 3 at sites 1, 2 and 3, and j = 1,2 for the upper and lower sonics respectively. (a) Site 3 lower (b) Site 1 upper, (c) Site 1 lower, (d) Site 2 upper, (e) Site 2 lower. The colours indicate thresholds

of the roof-top wind speed U_{ref}: ♦ U_{ref} < 1.1 m s^{-1}, ♦ 1.1 ≤ U_{ref} ≤ 2.5 m s^{-1}, and ♦ U_{ref} > 2.5 m s^{-1}. The blue curve on (e) is the fitted model of Dobre et al., 2005.

Fig. 5 Variation of sector-averaged (a) normalised vertical velocity (w/U_{ref}) and (b) cross street resultant wind speed, $(u^2 + w^2)^{0.5}$. ◊ U_{ref} < 1.1 m s^{-1}, □ 1.1 ≤ U_{ref} ≤ 2.5 m s^{-1}, and Δ U_{ref} > 2.5 m s^{-1}.

Fig. 6 - Wind vector roses at the intersection sites for θ_{ref} wind sectors centered on (a) 0° and (b) 180°. The colours indicate thresholds of the roof-top wind speed U_{ref}: ♦ U_{ref} < 1.1 m s^{-1}, ♦ 1.1 ≤ U_{ref} ≤ 2.5 m s^{-1}, and ♦ U_{ref} > 2.5 m s^{-1}. The length of each vector indicates the mean horizontal wind speed. The numerals 0.5 and 1, 1 and 2 and 2.5 and 5 on the inner and outer circles of the roses indicate wind speed values in m s^{-1}.

Fig. 7 (a,b) Wind vector roses at the intersection sites for θ_{ref} wind sectors centered on (a) 90° and (b) –90°. The colours indicate thresholds of the roof-top wind speed U_{ref}: ♦ U_{ref} < 1.1 m s^{-1}, ♦ 1.1 ≤ U_{ref} ≤ 2.5 m s^{-1}, and ♦ U_{ref} > 2.5 m s^{-1}. The length of each vector indicates the mean horizontal wind speed. The numerals 0.5 and 1, 1 and 2 and 2.5 and 5 on the inner and outer circles of the roses indicate wind speed values in m s^{-1}.

Fig. 8 Wind direction pdfs for 1 hour segments of 10 Hz data at the intersection sites for the near perpendicular θ_{ref} mean wind sectors centered on (a) 90° and (b) –90°. Top left: roof-top wind direction where legend indicates mean roof-top flow direction, bottom left: site layout with red arrow pointing in the direction of mean flow, top right: site 1 (lower sonic) and bottom right: site 2 (lower sonic).

Fig. 9 Superposition of Carpentieri et al. 2009 wind tunnel and flow visualization studies for θ_{ref} winds centred on 51.35° over a 1:200 scale model of the DAPPLE site. The vectors show the horizontal velocity field at z = 25 mm that corresponds to 5 m full scale. The photograph shows a dispersion realisation with source at

Gloucester Place and a horizontal light sheet at 20 mm in Marylebone Road showing a vortex at the eastsoutheast corner of the intersection.

Fig. 10 Wind vector roses at the intersection sites for θ_{ref} wind sectors centred on 60°. The colours indicate thresholds of the roof-top wind speed U_{ref}: ♦ U_{ref} < 1.1 m s^{-1}, ♦ 1.1 ≤ U_{ref} ≤ 2.5 m s^{-1}, and ♦ U_{ref} > 2.5 m s^{-1}. The length of each vector indicates the mean horizontal wind speed (see radial axes, in m s^{-1}).

Fig. 11 Wind direction pdfs for 1 hour segments of 10 Hz data at the intersection sites for the oblique θ_{ref} wind sector (45° ≤ θ_{ref} ≤ 75°). Top left: roof-top wind direction where legend indicates mean roof-top flow direction, bottom left: site layout with red arrow pointing in the direction of flow, top right: site 1 (lower sonic) and bottom right: site 2 (lower sonic).

Fig. 12 Wind vector roses at the intersection sites for θ_{ref} wind sectors centred on –120°. The colours indicate thresholds of the roof-top horizontal wind speed U_{ref}: ♦ U_{ref} < 1.1 m s^{-1}, ♦ 1.1 ≤ U_{ref} ≤ 2.5 m s^{-1}, and ♦ U_{ref} > 2.5 m s^{-1}. The length of each vector indicates the mean horizontal wind speed.

Fig. 13 Wind direction pdfs for 1 hour segments of 10 Hz data at the intersection sites for the oblique θ_{ref} wind sector (–105° ≤ θ_{ref} ≤ –135°). Top left: roof-top wind direction where legend indicates mean roof-top flow direction, bottom left: site layout with red arrow pointing in the direction of flow, top right: site 1 (lower sonic) and bottom right: site 2 (lower sonic).

Fig. 14 Schematic illustration of observed flow features at and around the intersection for fluctuating oblique roof-top flow.

Fig. 15 Variation of sector-averaged in-street vertical wind angle (γ) with θ_{ref} (a) Site 1 upper, (b) Site 1 lower, (c) Site 2 upper and (d) Site 2 lower. ◊ U_{ref} < 1.1 m

s^{-1}, □ $1.1 \leq U_{ref} \leq 2.5$ m s^{-1}, and Δ $U_{ref} > 2.5$ m s^{-1}. Error bars are $\pm 1\sigma$ based on sector averages of 15 minute data.

.

colour figure

Click here to download colour figure: Fig1a.ppt

Fig1a

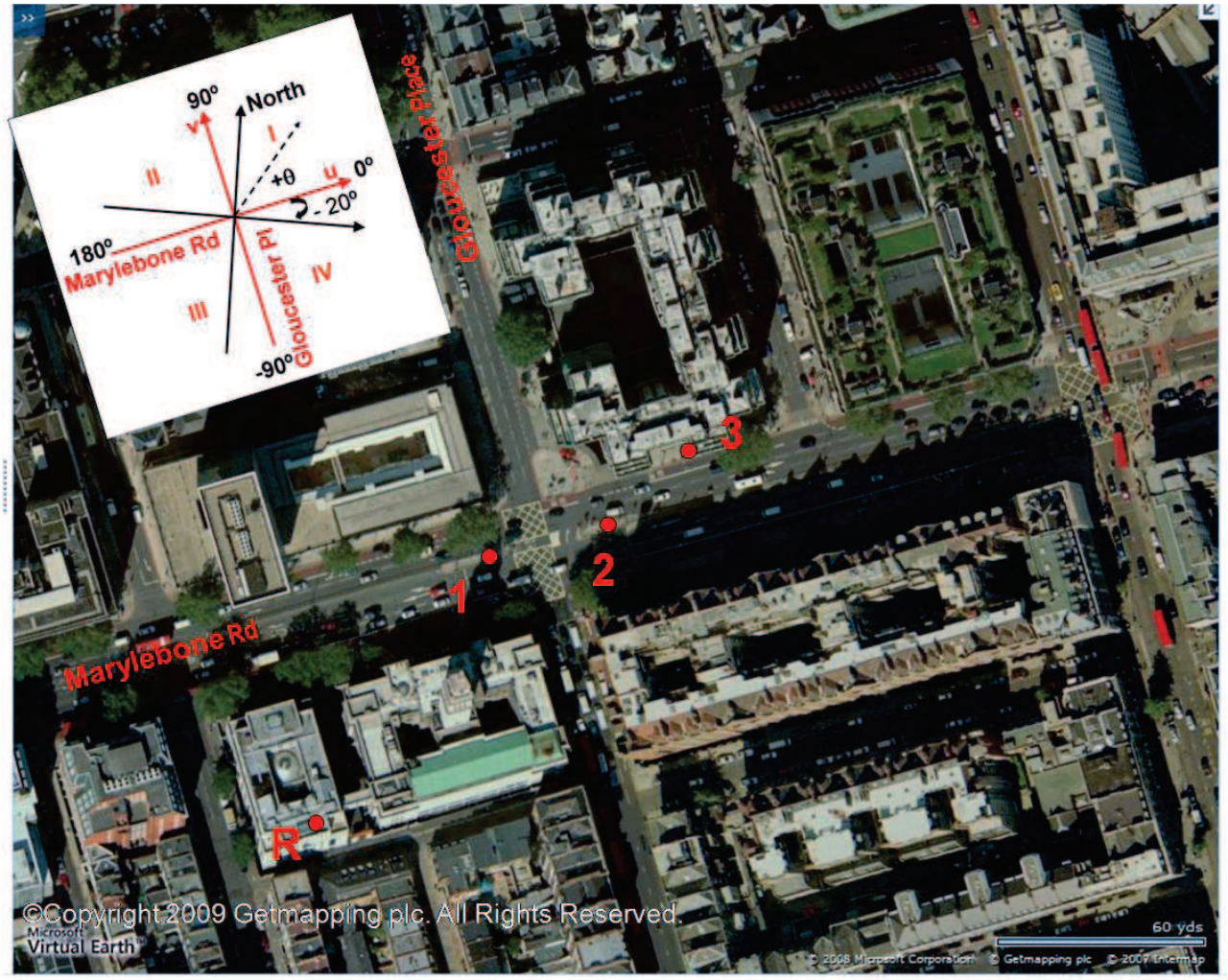

colour figure

Click here to download colour figure: Fig1b.ppt

Fig1b

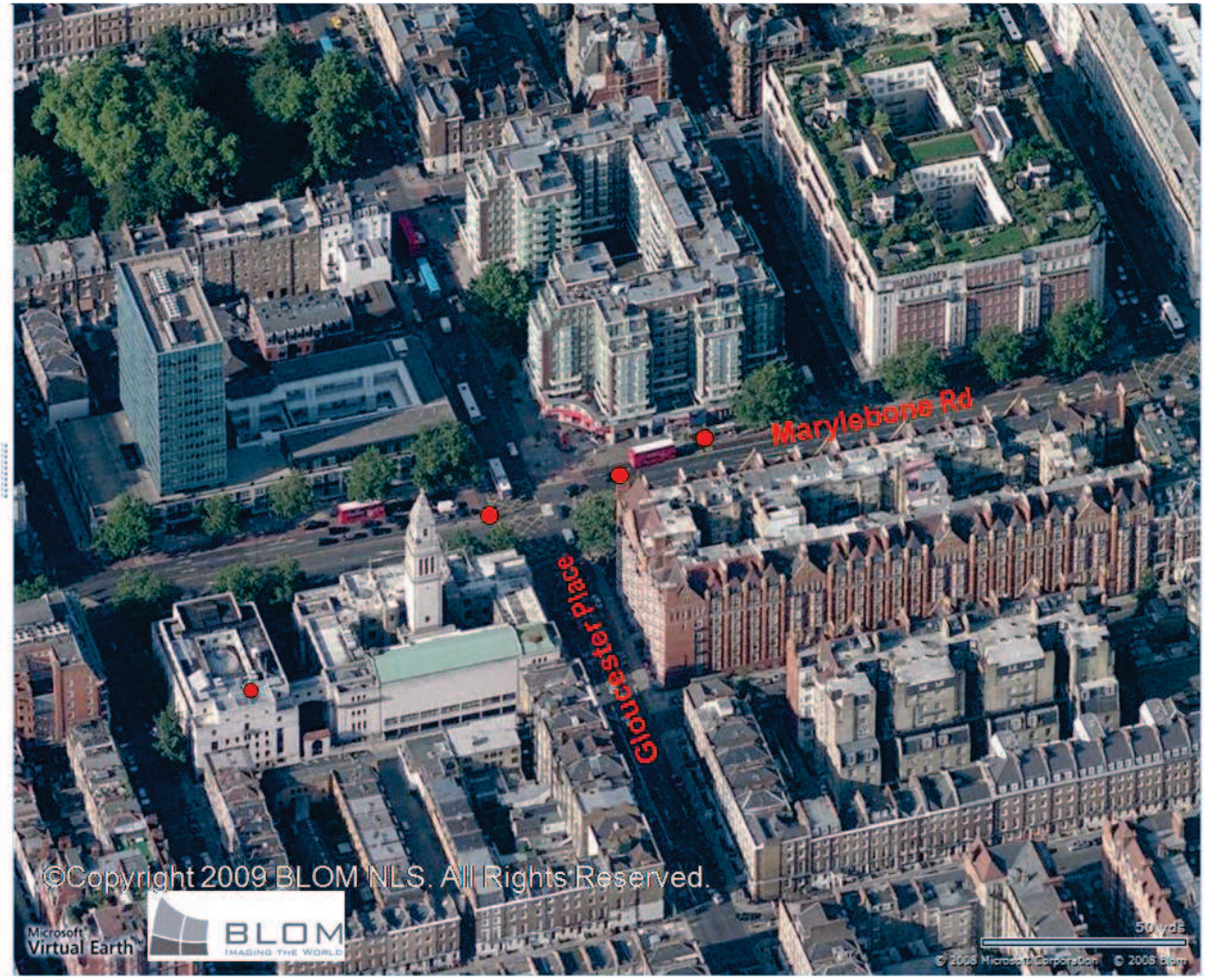

colour figure

Click here to download colour figure: Fig2.ppt

Fig2

colour figure

Click here to download colour figure: Fig3.ppt

Fig. 3

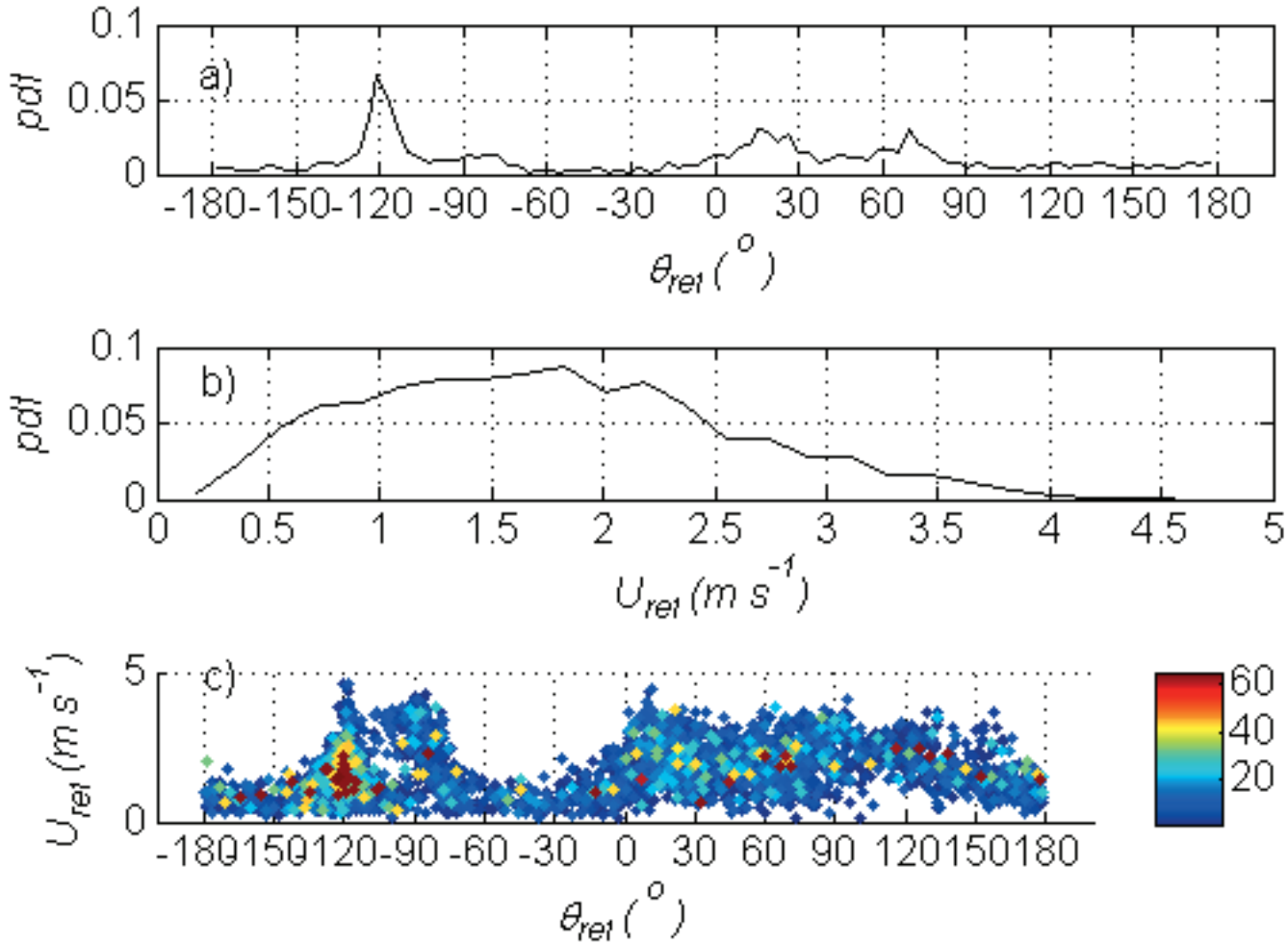
a)
pdf
0.1
0.05
0
-180 -150 -120 -90 -60 -30 0 30 60 90 120 150 180
θ_{rel} (^{o})
b)
pdf
0.1
0.05
0
0 0.5 1 1.5 2 2.5 3 3.5 4 4.5 5
U_{rel} ($m\ s^{-1}$)
c)
U_{rel} ($m\ s^{-1}$)
5
0
-180 -150 -120 -90 -60 -30 0 30 60 90 120 150 180
θ_{rel} (^{o})
60
40
20

colour figure

Click here to download colour figure: Fig4a.ppt

Fig. 4a

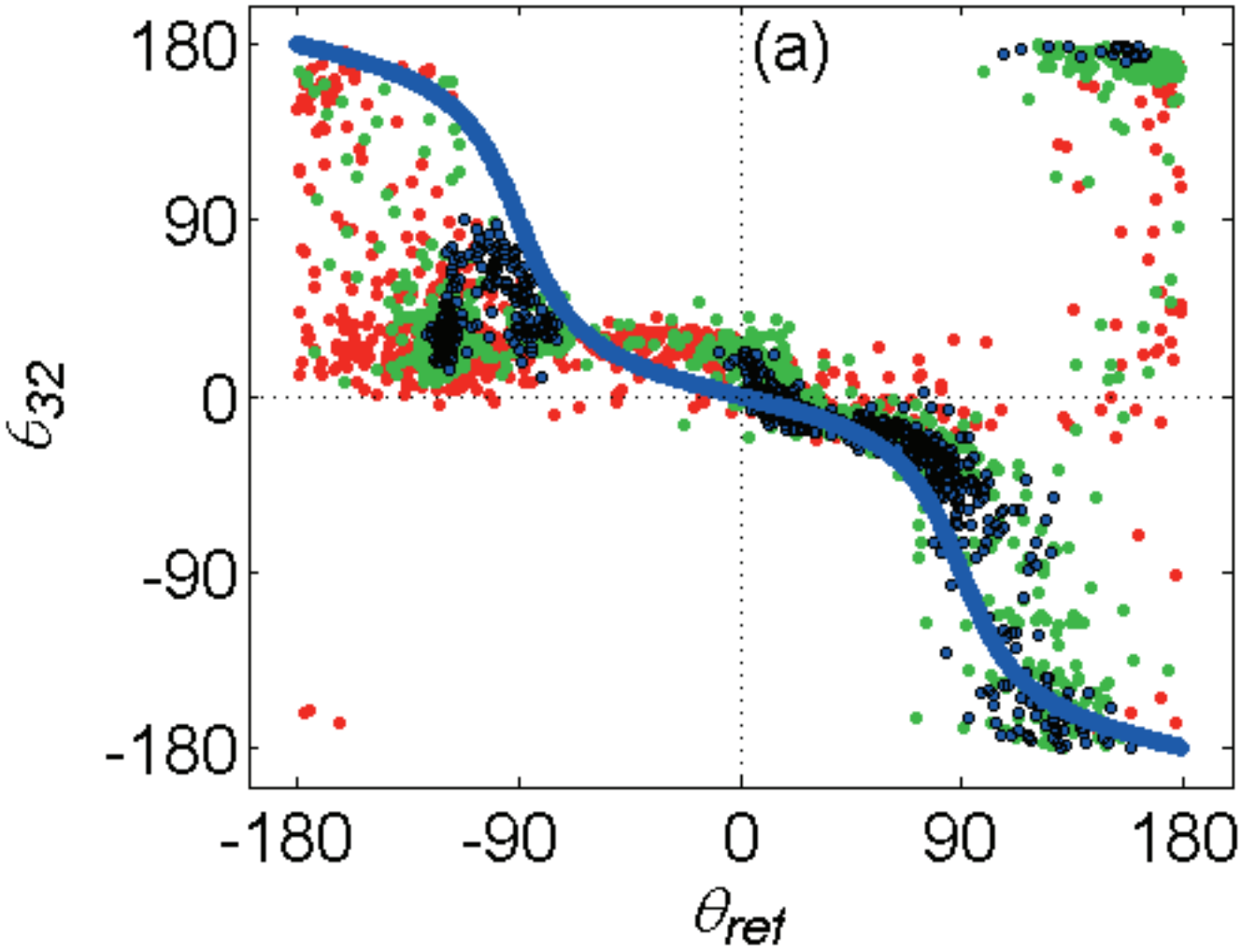

colour figure

Click here to download colour figure: Fig4b.ppt

Fig.4b

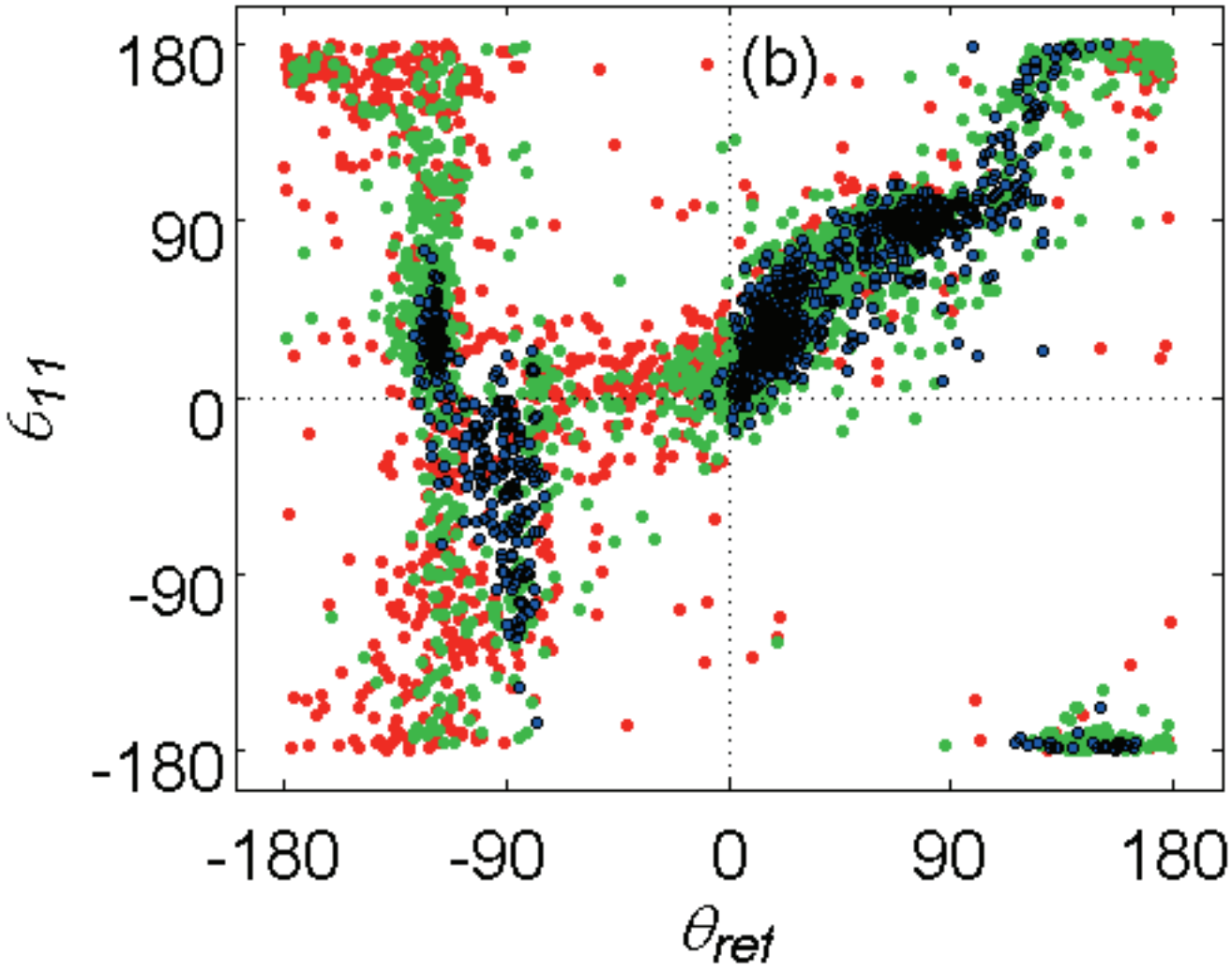

colour figure

Click here to download colour figure: Fig4c.ppt

Fig. 4c

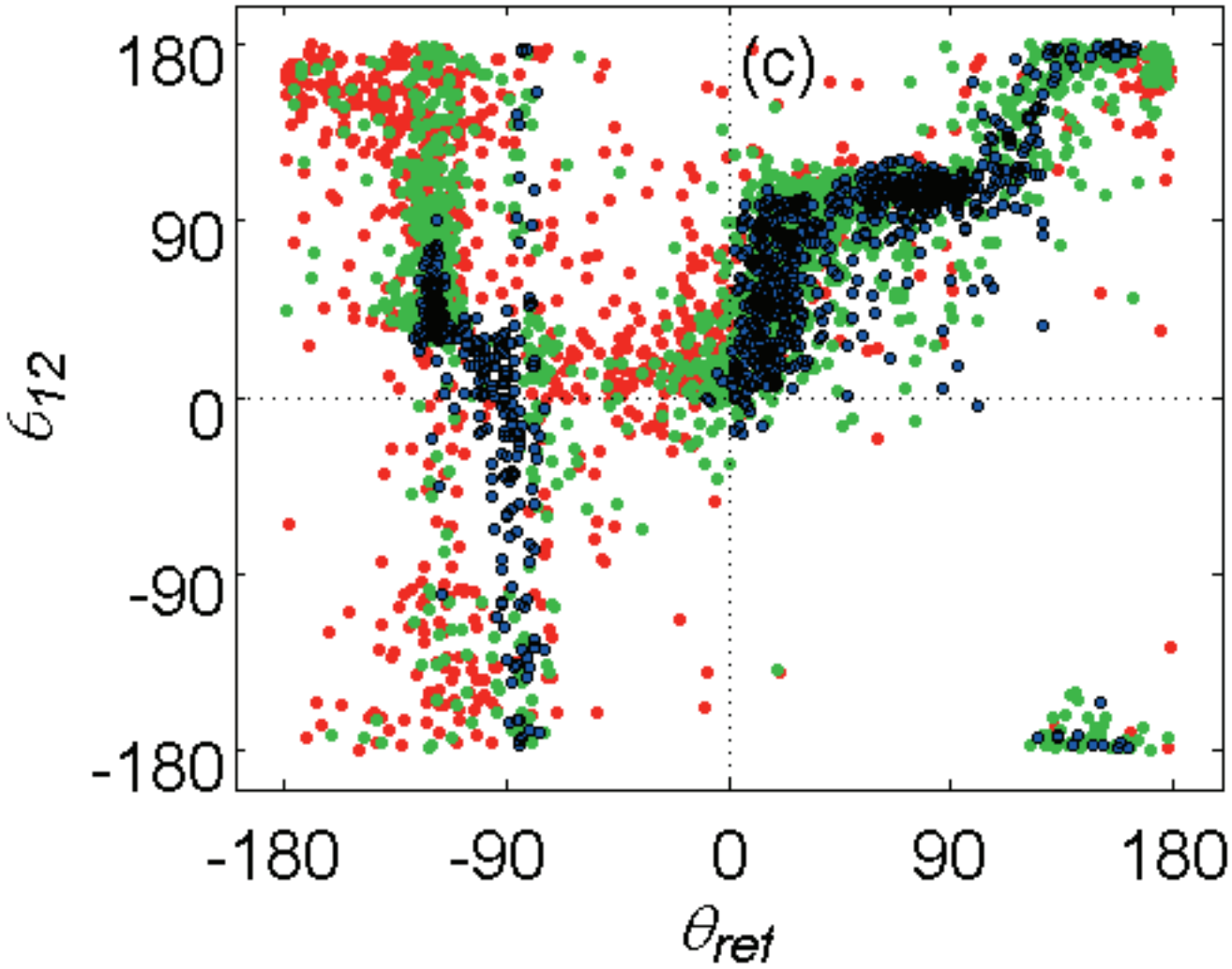

colour figure
Click here to download colour figure: Fig4d.ppt

Fig. 4d

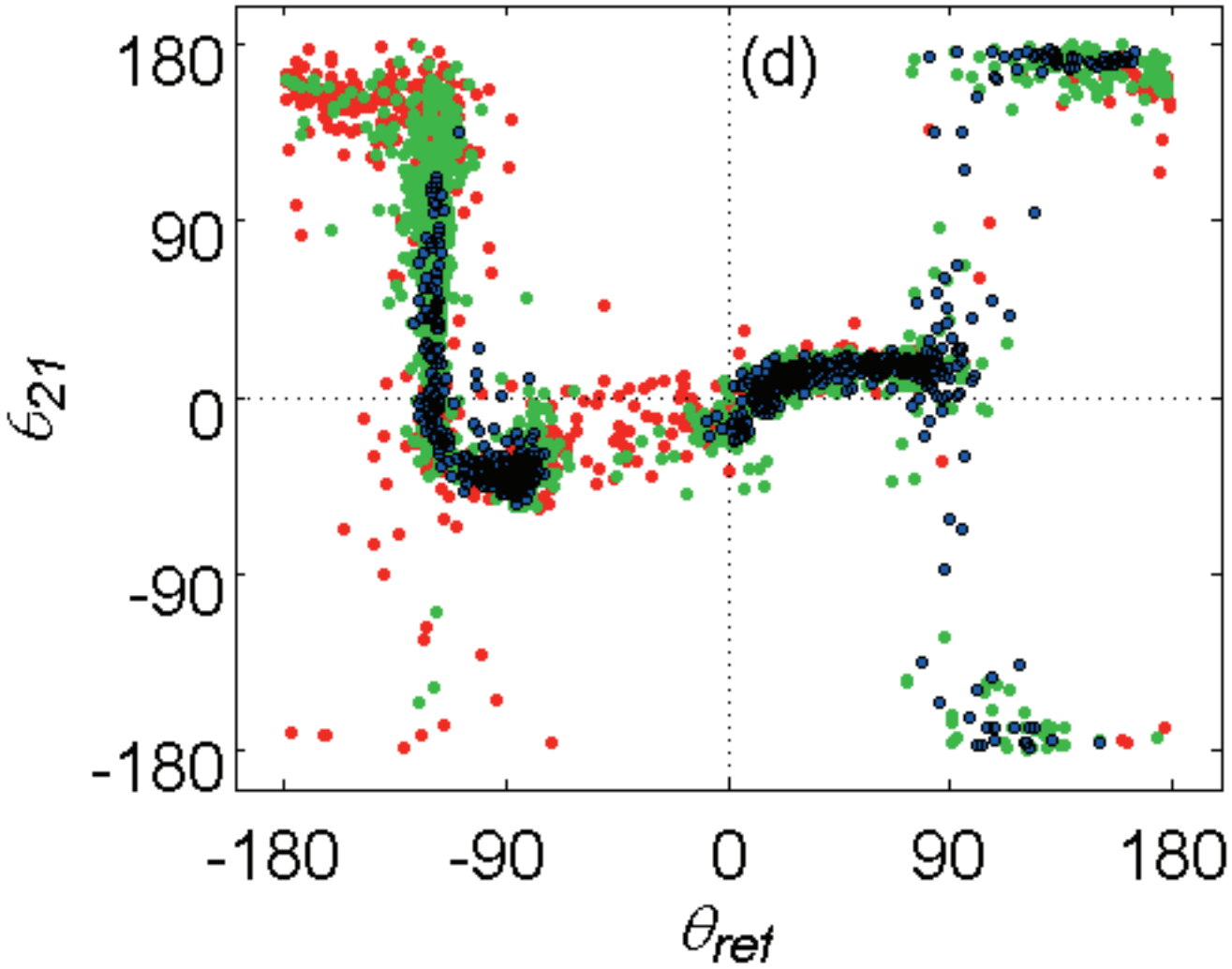

colour figure

Click here to download colour figure: Fig4e.ppt

Fig. 4e

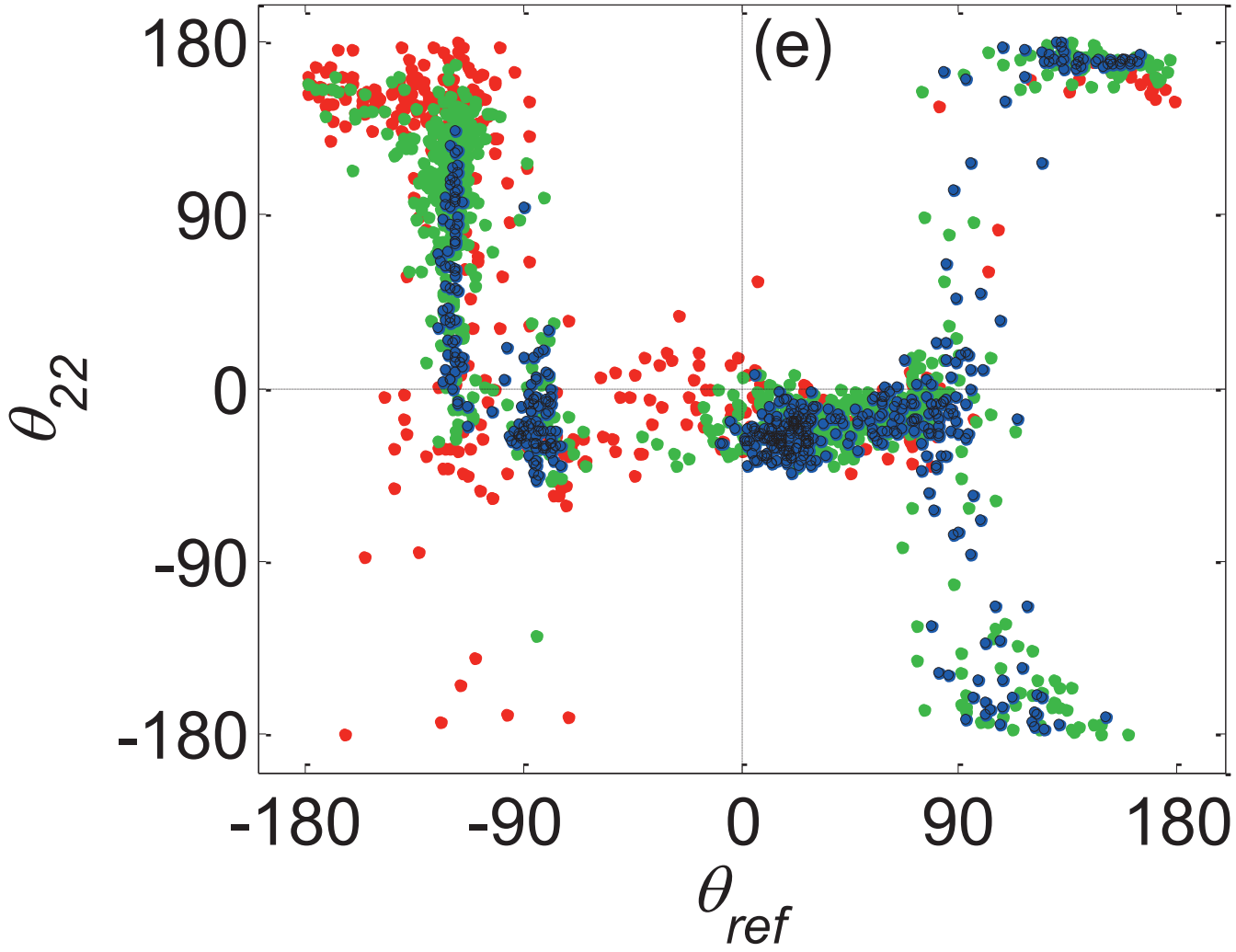

line figure
Click here to download line figure: Fig5.ppt

Fig. 5

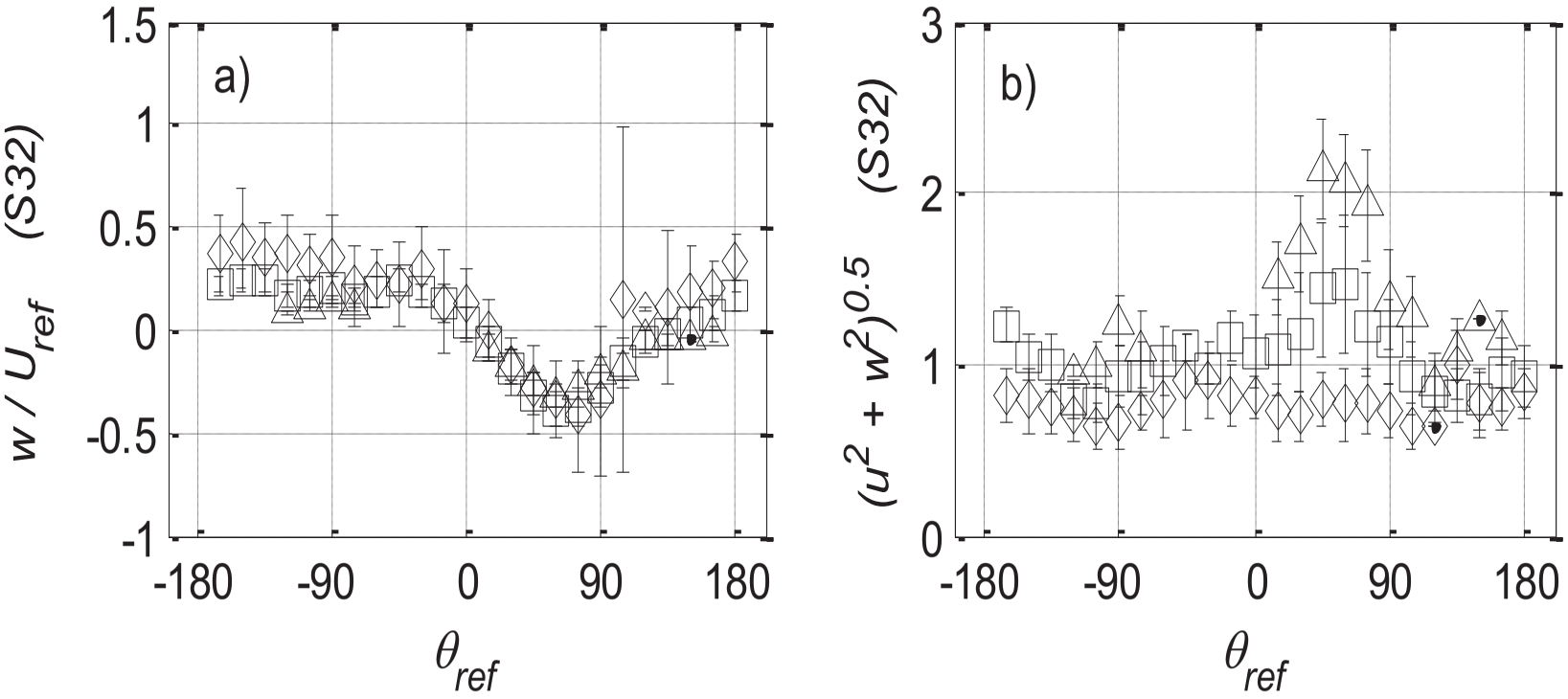

colour figure

Click here to download colour figure: Fig6a.ppt

Fig. 6a

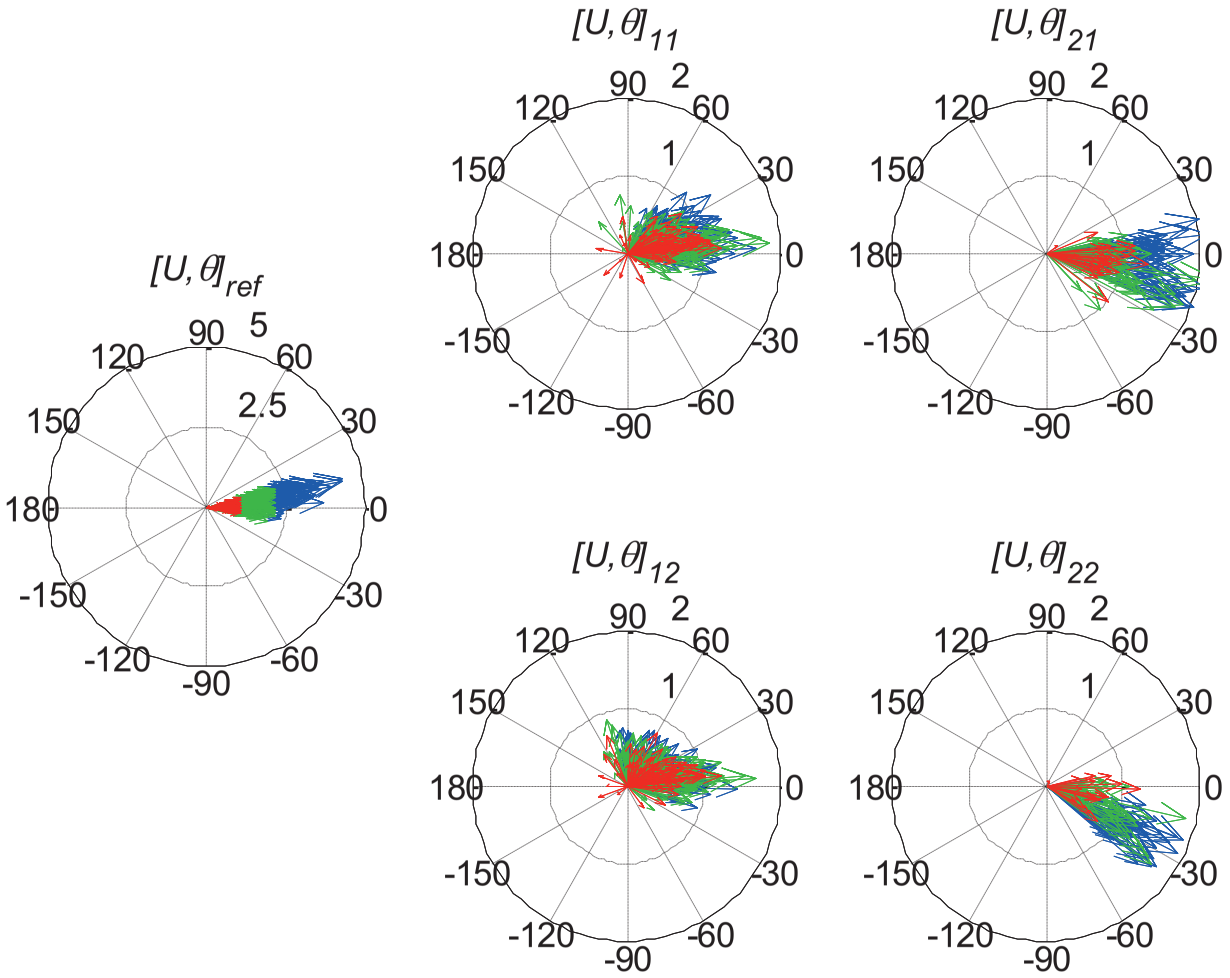

colour figure

Click here to download colour figure: Fig6b.ppt

Fig. 6b

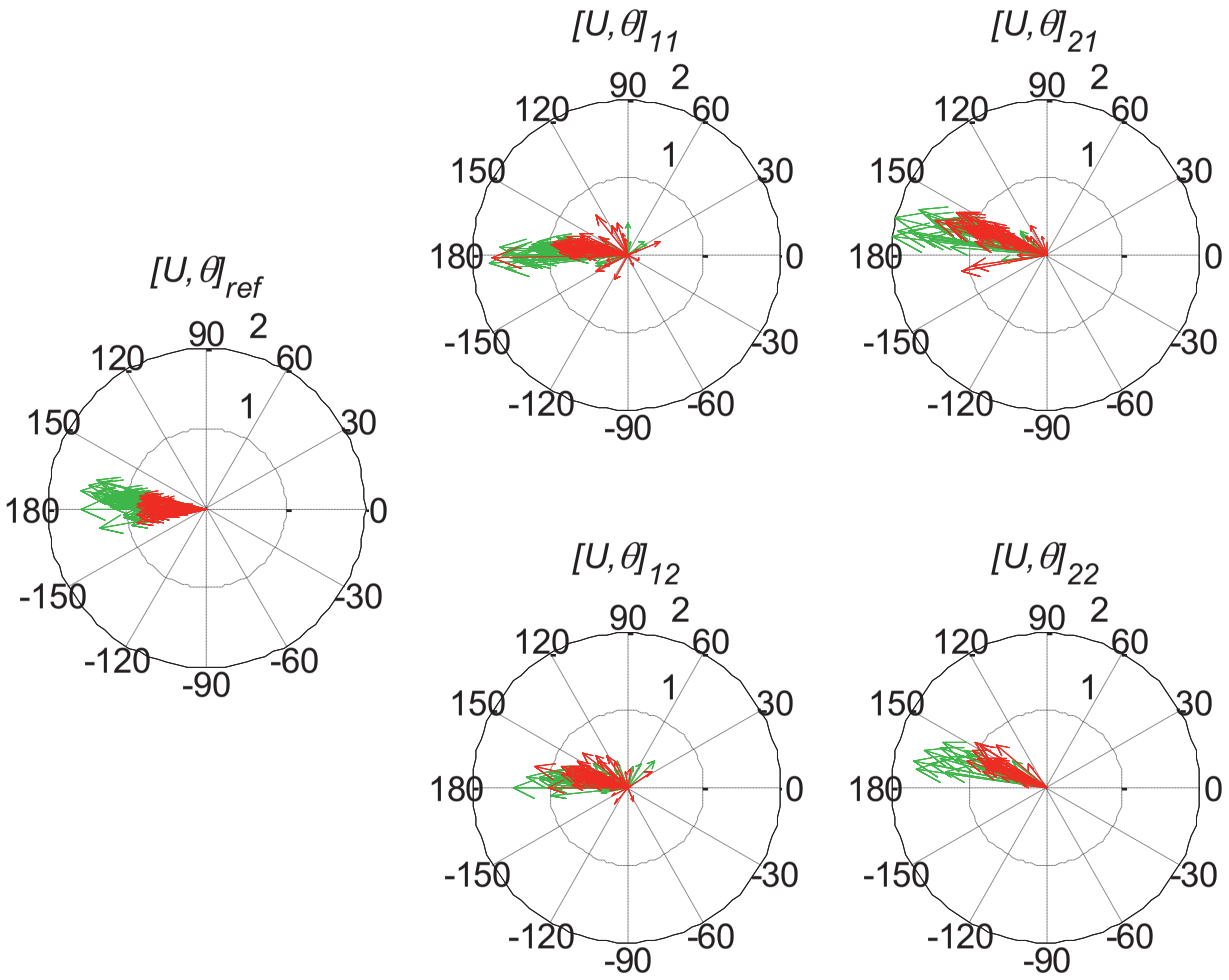

colour figure

Click here to download colour figure: Fig7a.ppt

Fig. 7a

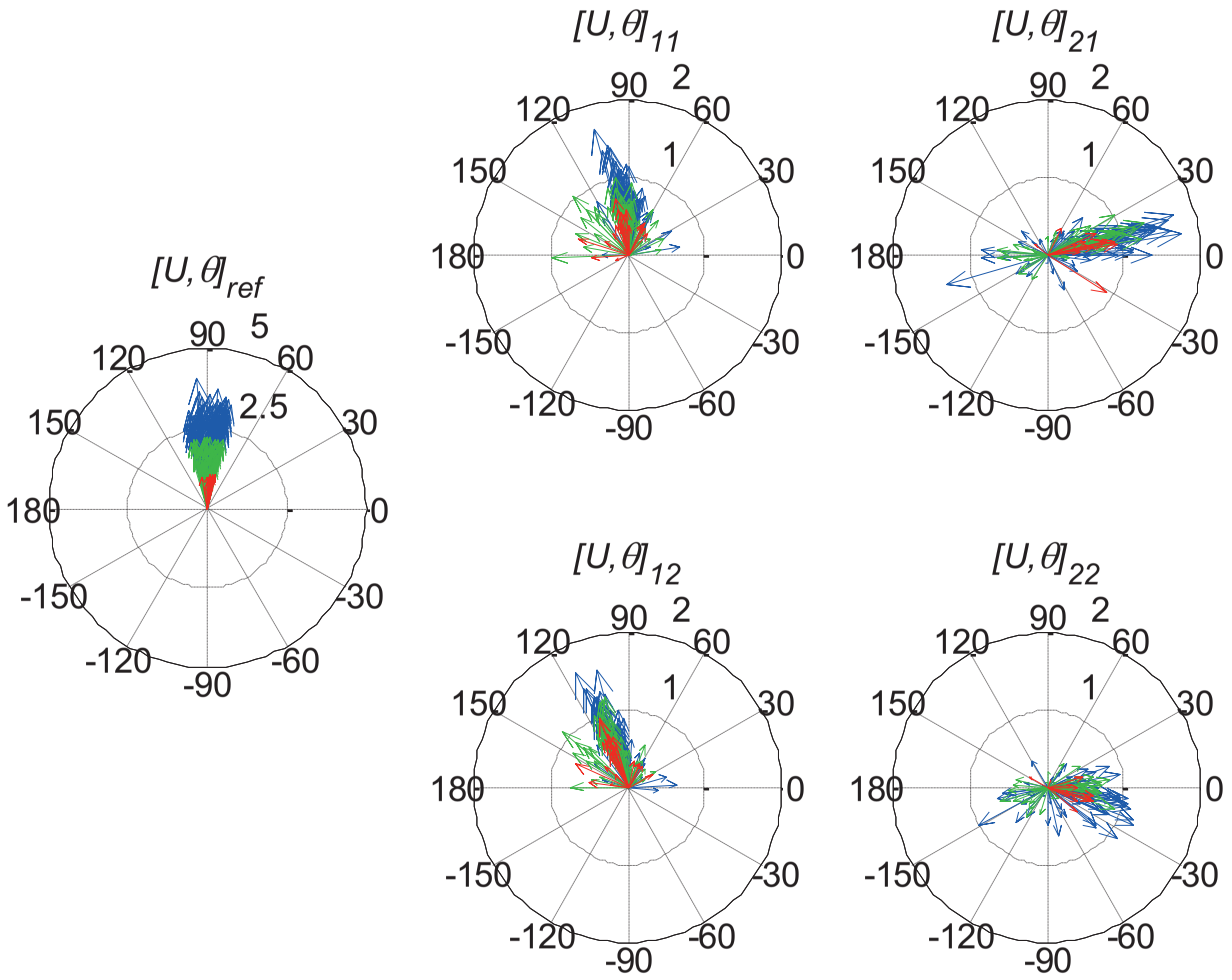

colour figure

Click here to download colour figure: Fig7b.ppt

Fig. 7b

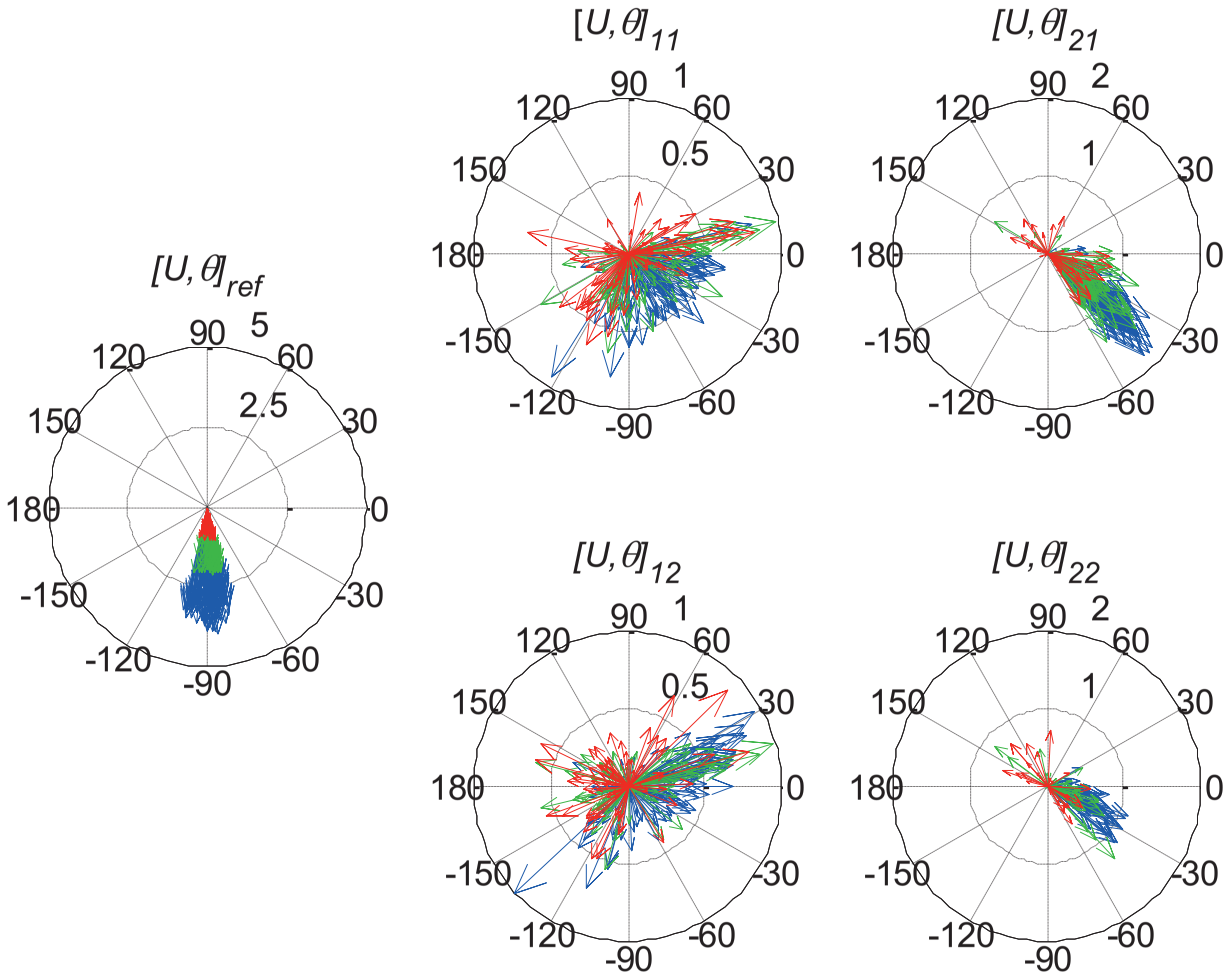

colour figure
Click here to download colour figure: Fig8a.ppt

Fig. 8a

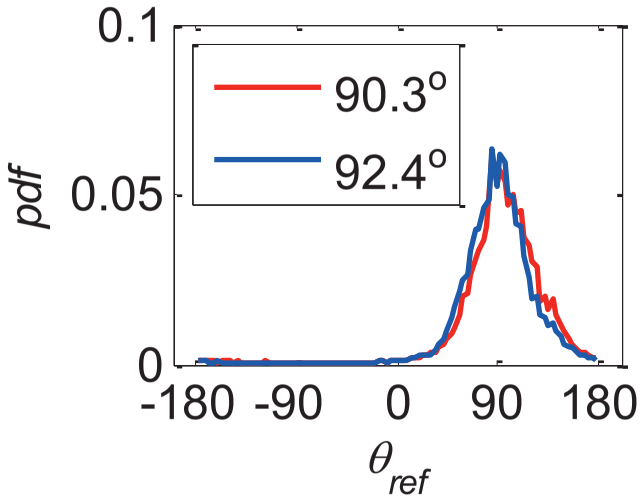

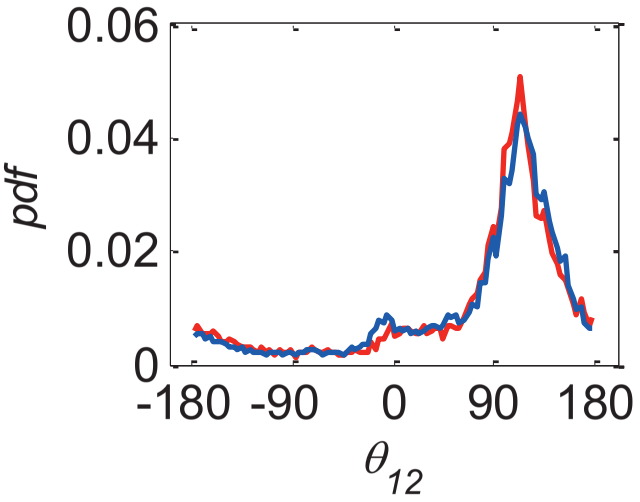

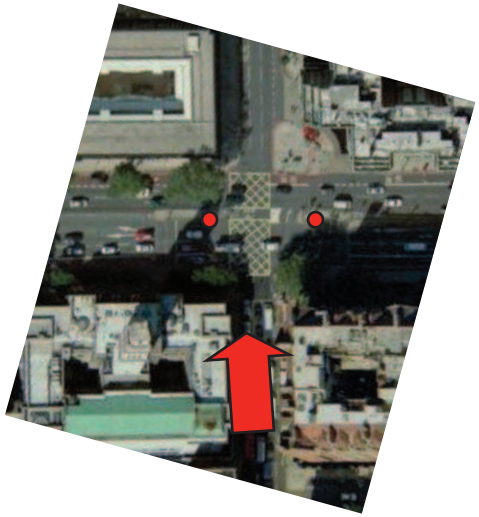

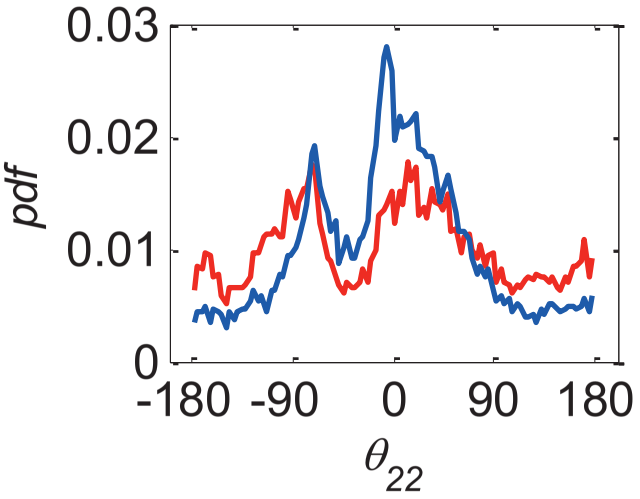

colour figure

Click here to download colour figure: Fig8b.ppt

Fig. 8b

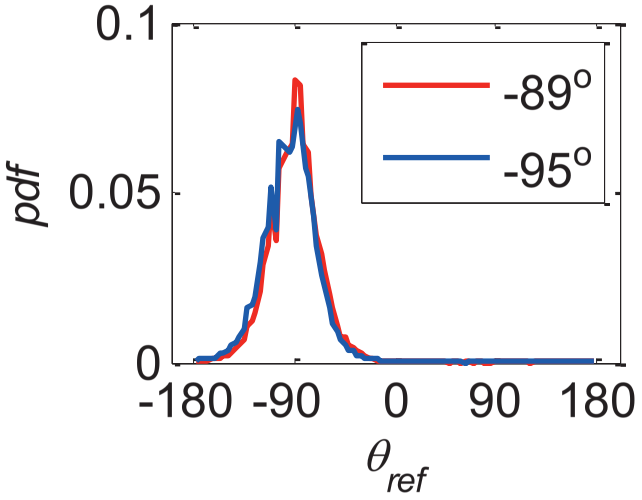
0.1
0.05
0
pdf
-89°
-95°
-180 -90 0 90 180
θ_{ref}

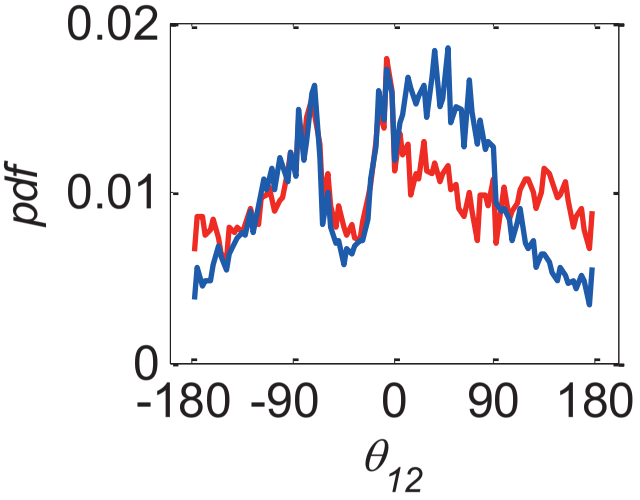
0.02
0.01
0
pdf
-180 -90 0 90 180
θ_{12}

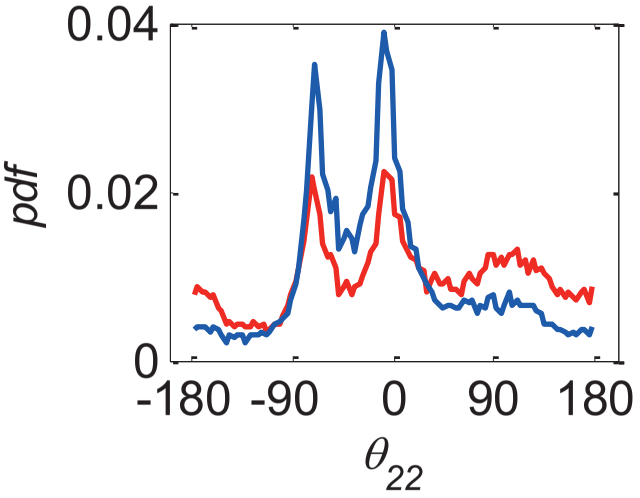
0.04
0.02
0
pdf
-180 -90 0 90 180
θ_{22}

colour figure

Click here to download colour figure: Fig9.ppt

Fig. 9

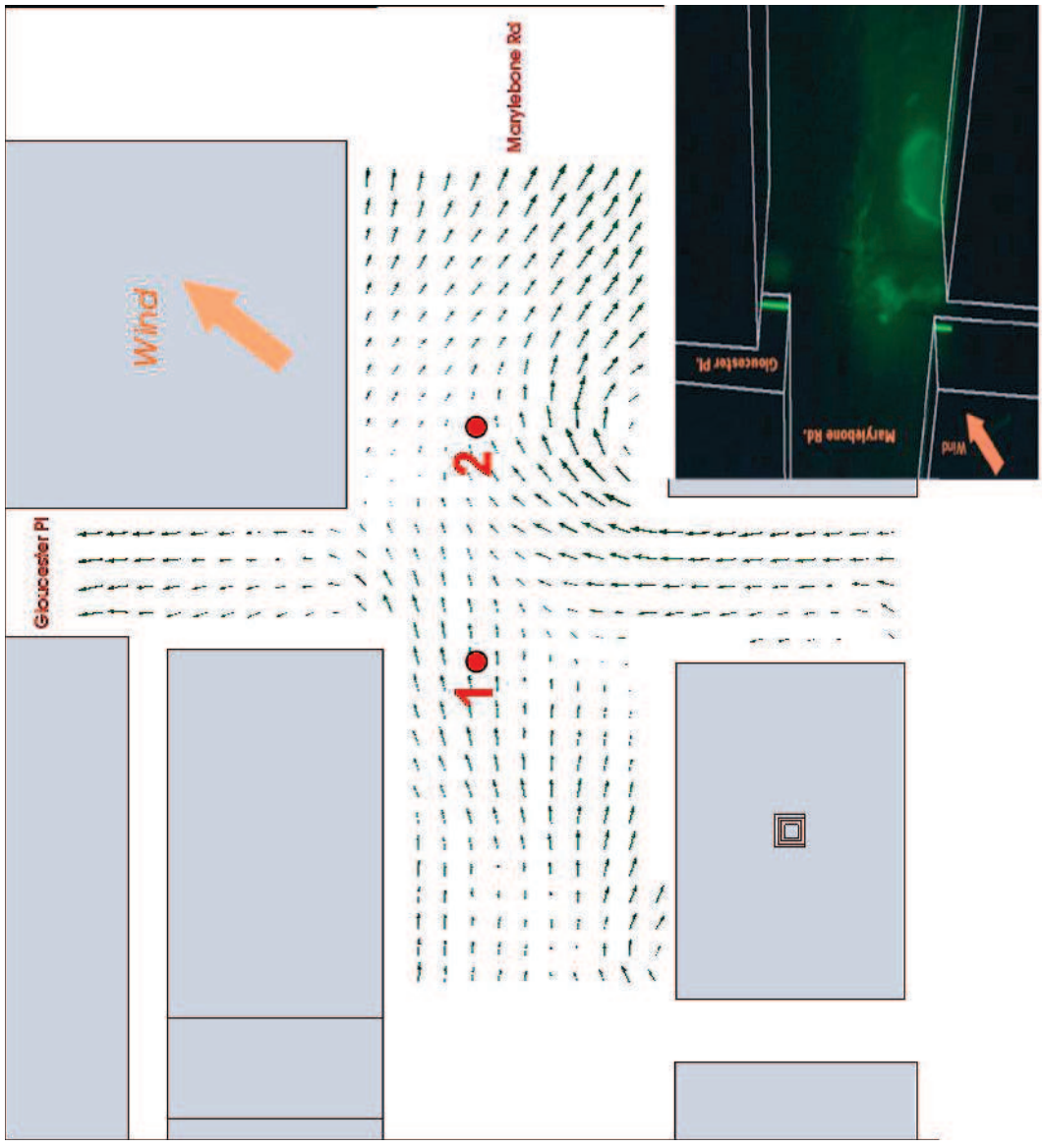
Marylebone Rd
Wind
Gloucester Pl
1
2
Gloucester Pl.
Marylebone Rd.
Wind

colour figure

Click here to download colour figure: Fig10.ppt

Fig. 10

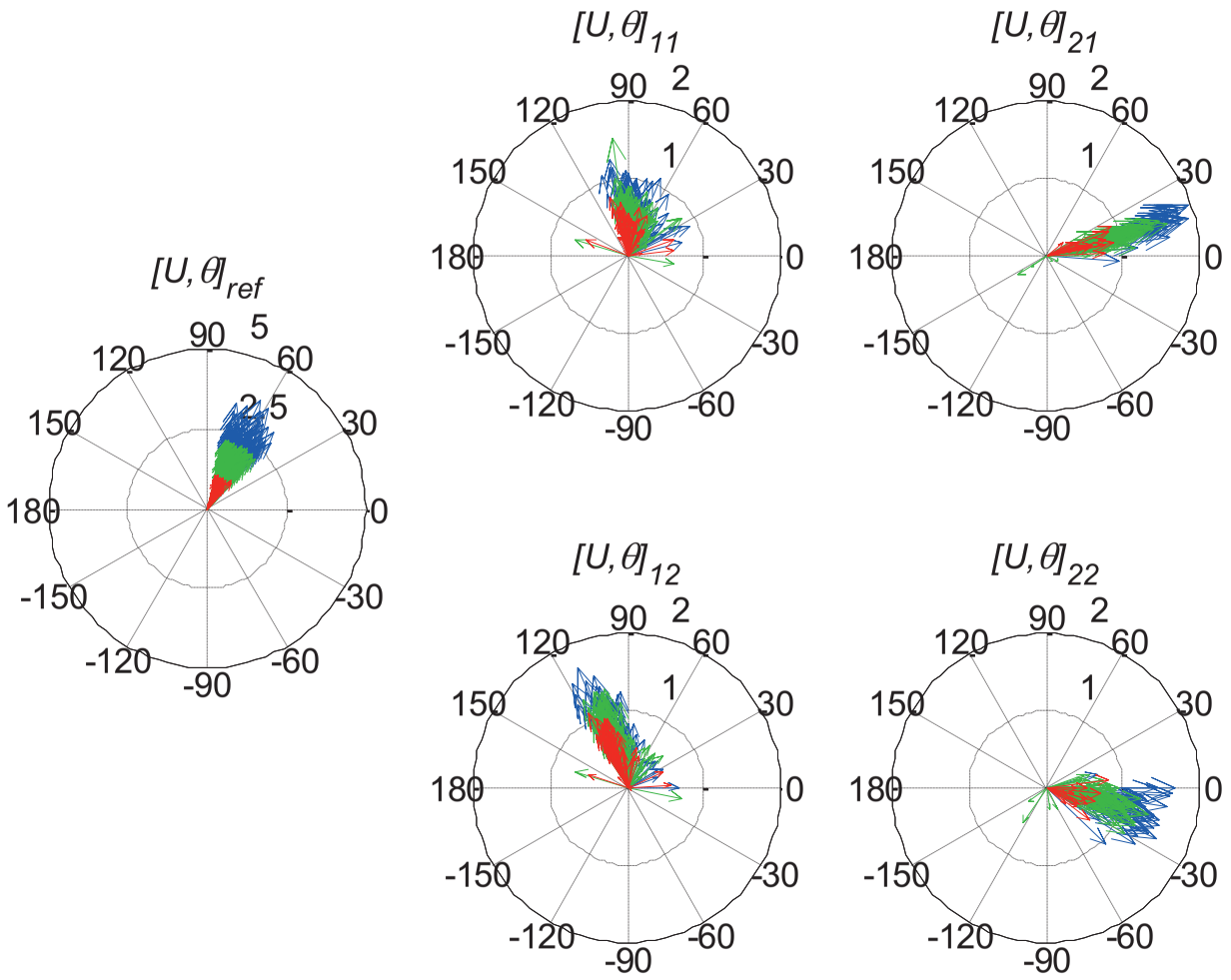

colour figure
Click here to download colour figure: Fig11.ppt

Fig. 11

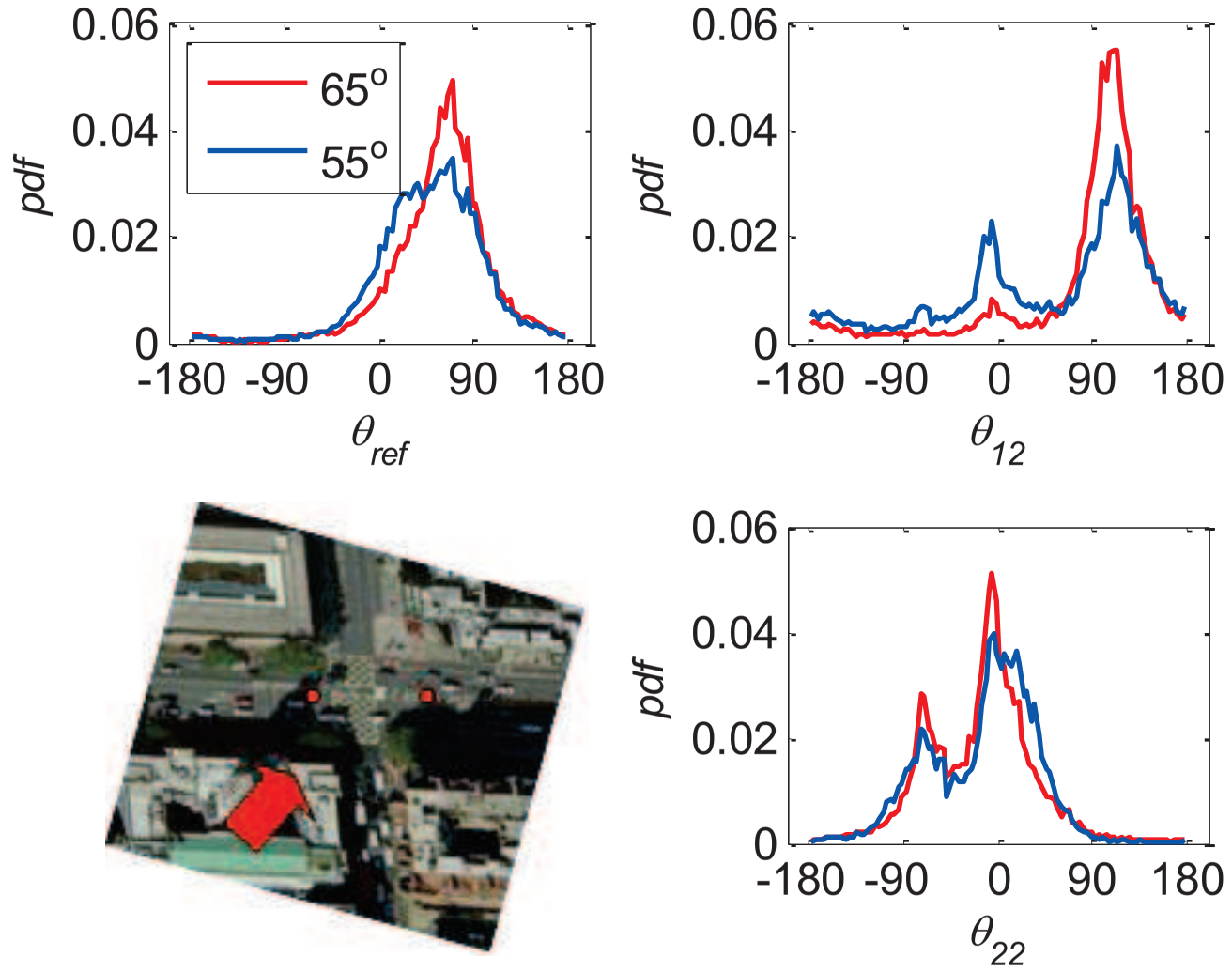

colour figure

Click here to download colour figure: Fig12.ppt

Fig. 12

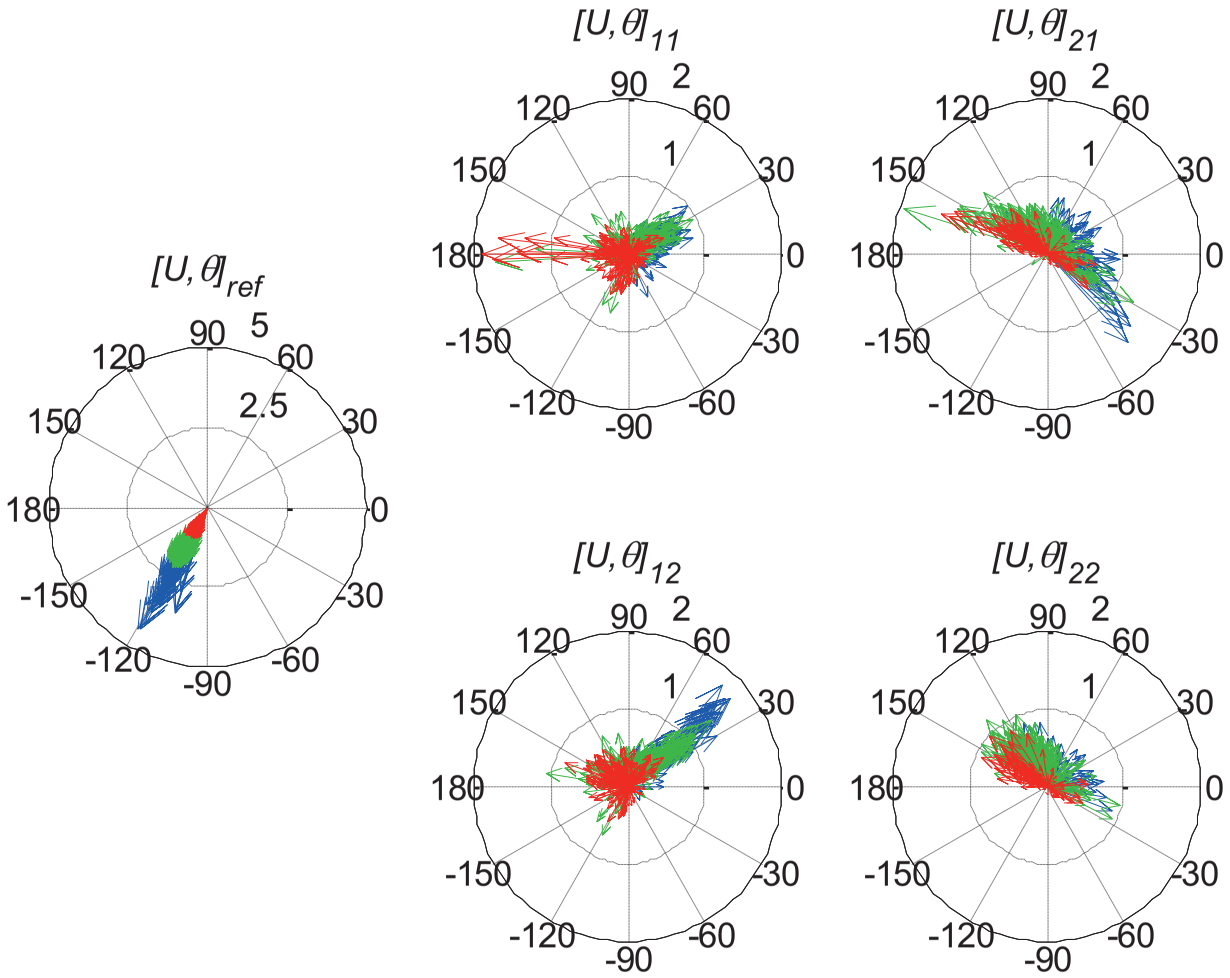

colour figure
Click here to download colour figure: Fig13.ppt

Fig. 13

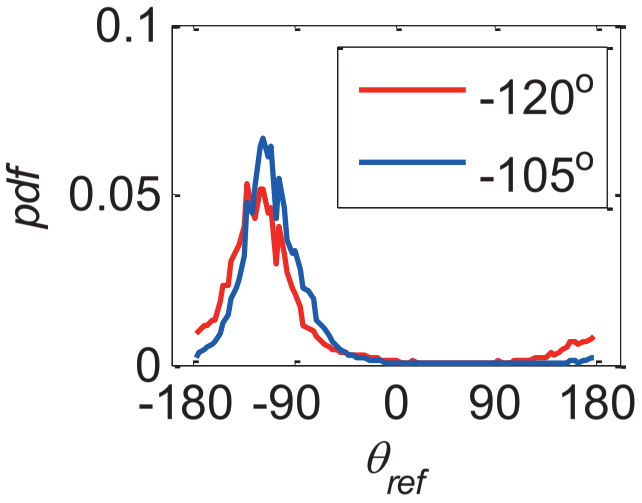

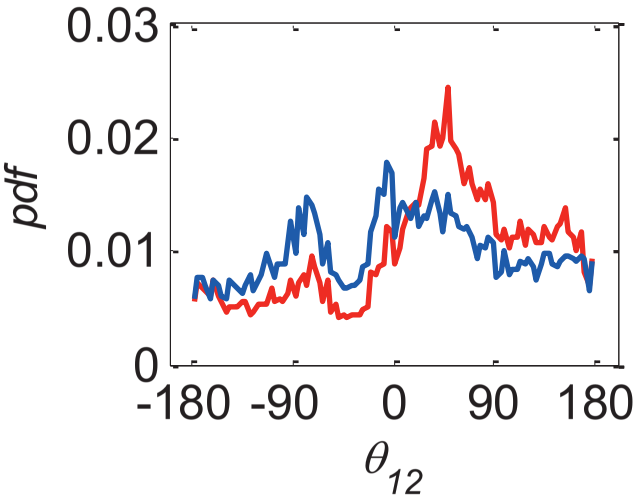

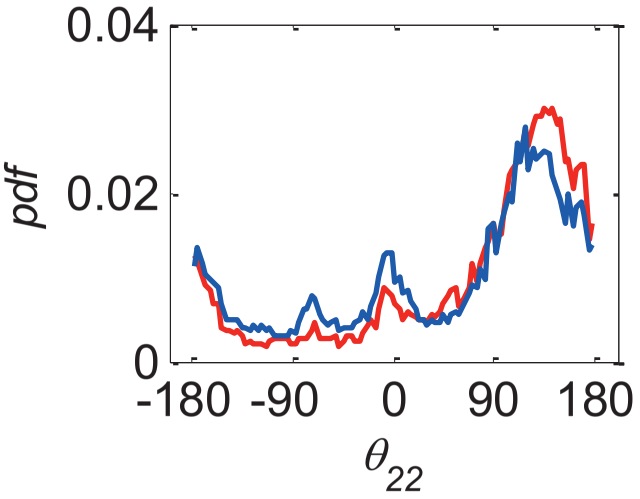

colour figure
Click here to download colour figure: Fig14.ppt

Fig. 14

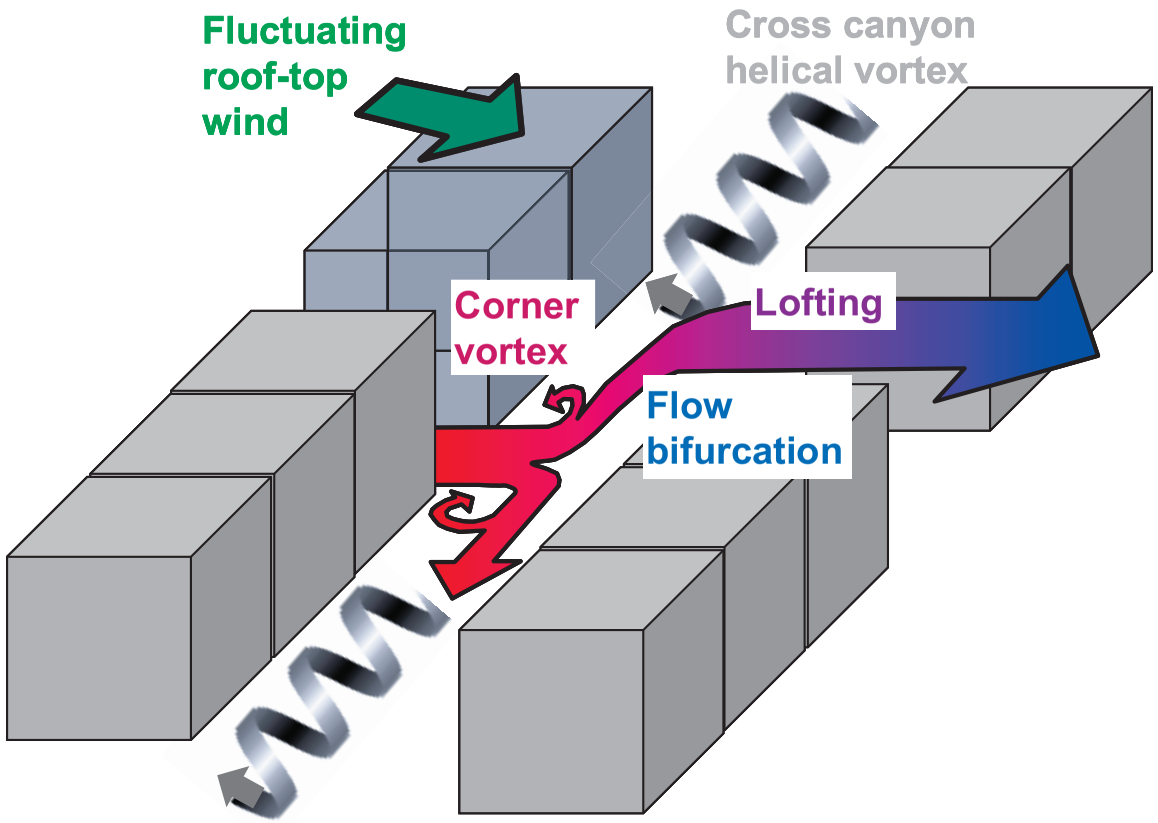

line figure
Click here to download line figure: Fig15.ppt

Fig. 15